PREDICTION OF LONG-TERM CREEP BEHAVIOR OF EPOXY ADHESIVES FOR STRUCTURAL APPLICATIONS

A Thesis

by

CHIH-WEI FENG

Submitted to the Office of Graduate Studies of
Texas A&M University
in partial fulfillment of the requirements for the degree of

MASTER OF SCIENCE

August 2004

Major Subject: Mechanical Engineering

PREDICTION OF LONG-TERM CREEP BEHAVIOR OF

EPOXY ADHESIVES FOR STRUCTURAL APPLICATIONS

A Thesis

by

CHIH-WEI FENG

Submitted to Texas A&M University
in partial fulfillment of the requirements
for the degree of

MASTER OF SCIENCE

Approved as to style and content by:

Hung-Jue Sue (Chair of Committee)	Abraham Clearfield (Member)
C. Steve Suh (Member)	Dennis O'Neal (Head of Department)

August 2004

Major Subject: Mechanical Engineering

ABSTRACT

Prediction of Long-Term Creep Behavior of Epoxy Adhesives

for Structural Applications. (August 2004)

Chih-Wei Feng, B.S., National Taiwan University, Taipei, Taiwan

Chair of Advisory Committee: Dr. Hung-Jue Sue

The mechanical property of polymeric materials changes over time, especially when they are subjected to long-term loading scenarios. To predict the time-dependent viscoelastic behaviors of epoxy-based adhesive materials, it is imperative that reliable accelerated tests be developed to determine their long-term performances under different exposed environments. A neat epoxy resin system and a commercial structural adhesive system for bonding aluminum substrates are investigated. A series of moisture diffusion tests have been performed for more than three months in order to understand the influence of the absorbed moisture on creep behavior. The material properties, such as elastic modulus and glass transition temperature, are also studied under different environmental conditions. The time-temperature superposition method

produces a master curve allowing the long-term creep compliance to be estimated. The physics-based Coupling model is found to fit well the long-term creep master curve. The equivalence of the temperature and moisture effect on the creep compliance of the epoxy adhesives is also addressed. Finally, a methodology for predicting the long-term creep behavior of epoxy adhesives is proposed.

ACKNOWLEDGEMENTS

The author is grateful to Dr. H.-J. Sue for his guidance and endless support and especially for his help in overcoming some critical problems during the last two years. Dr. Sue also provided a great experimental environment to assist the author to work more independently. The author also would like to thank his committee members, Dr. Clearfield and Dr. Suh, for their commitment to this research.

The author wishes to thank Dr. Y.-Y. Wang of Dow Automotive for the supply of epoxy adhesive materials and his endless guidance for the use of epoxy adhesives for this research. The author also appreciates the assistance of a portion of DMA tests from Mr. J. Huang of Dow Chemical. A particular thank you is given to Dr. Griffin for his attendance at the final defense.

Finally, the author would like to thank the friends and family who have supported him through these years of study with care and understanding. Special thanks are extended to the author's father and mother for instilling since childhood their belief in the importance of education.

TABLE OF CONTENTS

Page

CHAPTER Page

LIST OF FIGURES

FIGURE Page

FIGURE Page

LIST OF TABLES

CHAPTER I

INTRODUCTION

Background

Structural adhesives are load-bearing joining materials with high modulus and strength, and can help maintain structural integrity of multi-component parts via uniform transmission of stresses between them. The science and technology of polymeric adhesives did not emerge until a couple of decades ago [1]. Additionally, thanks to the availability of a variety of additives and catalysts, the polymeric adhesives today can meet various application needs of industries.

A driving force for the development and growth in the adhesives market is the exceptional advantages offered compared with the traditional joining techniques, such as riveting, bolting or welding. The advantages that adhesives can offer include: an improved stress distribution, an ability to join dissimilar parts, preservation of the material integrity, design flexibility and cost-effectiveness. Besides, the unique viscoelastic properties of polymeric adhesives can minimize vibration, which is especially attractive for the aerospace or automobile applications.

However, being viscoelastic in nature, polymeric materials exhibit unique time-dependent behaviors. This leads to a general concern in using structural adhesives extensively mainly due to the lack of long-term service life database and nearly nonexistent theory/model that can reliably predict viscoelastic behavior of polymers.

This thesis follows the style of Materials Science and Engineering A.

Furthermore, adhesive materials are expected not only to carry the service loads but also to sustain environmental aging. Hence, the inevitable coupled effects of the surroundings also need to be considered during service.

Epoxy resins would be the focused materials here because of their high strength-to-weight ratio, excellent adhesion to many surfaces, superior thermal stability, ease of processing and durability. A neat epoxy-based material and a commercial adhesive product are chosen to study at the same time for this research.

Objective and Scope

A brief overview for the framework of this project has been shown in Fig. 1.1. The key factors that affect the long-term durability of the epoxy resins are discussed first. A proper curing schedule is determined to achieve the fully-cured structural network for each system. Each transition temperature is measured as a guide for deciphering different scales of molecular motions and also as a reference testing temperature range. Isochronous creep tests at different applied loads are manipulated to validate the stress level in the linearly viscoelastic region. Then, the inevitable temperature and moisture effects on the material properties of epoxy adhesives are also investigated. Short-term creep experiments at elevated temperatures and/or with saturated moisture absorption are conducted to modify the performance in service environments. Finally, the temperature-moisture equivalence is adjusted and a predictive model is utilized to interpret the long-term creep behavior based on the time-temperature superposition principle.

In summary, the approaches included determining the mechanical behaviors of epoxy-based adhesives by using reliable accelerated tests and utilizing a physics-based model to predict the long-term behaviors under various environmental conditions. In the end, the objective to establish a methodology which is capable to evaluate the service-life performance of epoxy-based adhesives can be accomplished.

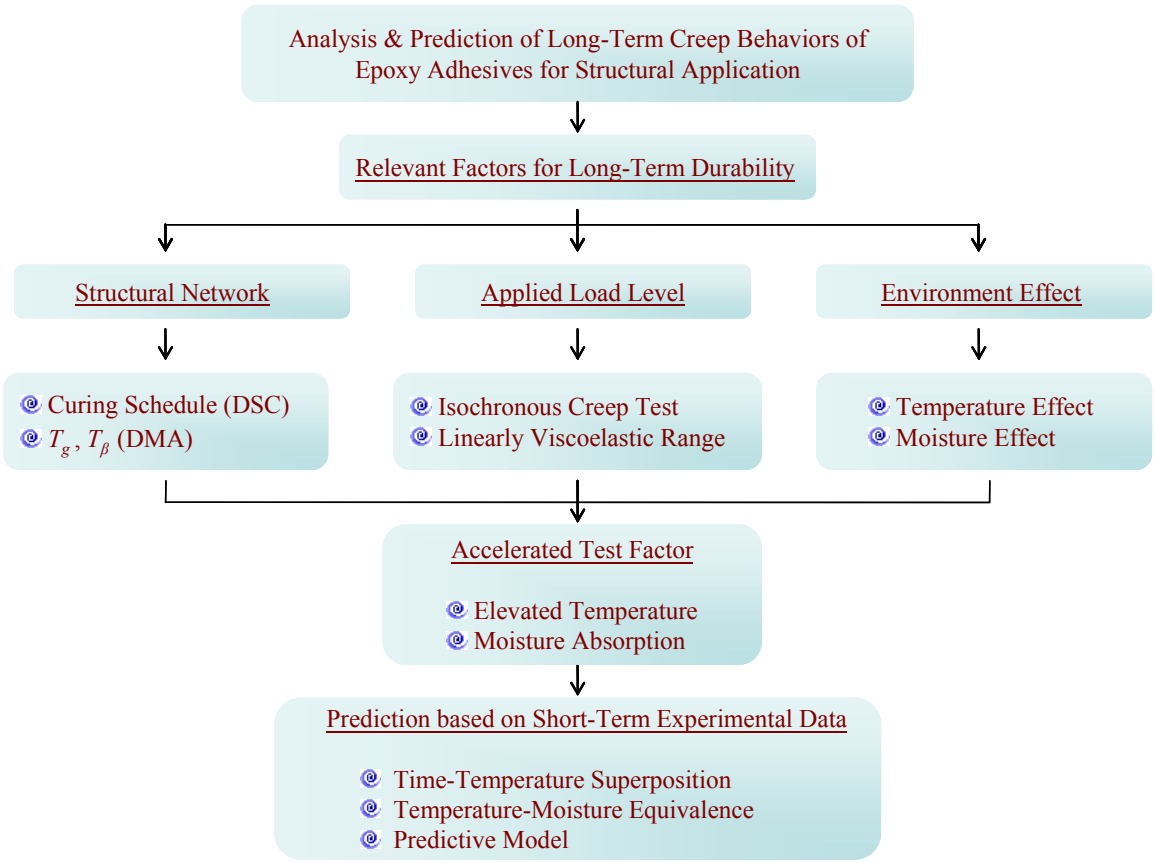

Fig. 1.1. The outline of the research for analysis and prediction of long-term behaviors of epoxy adhesives.

CHAPTER II

LITERATURE REVIEW

This chapter gives background information of the issues related to this research. First, the influences of stress, temperature and moisture on viscoelastic behaviors of polymers are addressed. The second section reviews the previous efforts in modeling the viscoelastic behaviors. Finally, a predictive model for describing the viscoelastic responses under the coupled stress and environmental effects are discussed.

Stress Effect

The creep spectrum is stress-dependent when the stress level is increased from linearly to nonlinearly viscoelastic region [2, 3]. In the linearly viscoelastic region, the creep strain is a linear function of stress, which means the creep compliance is independent of applied stress levels. Polymeric materials generally exhibit linearly viscoelastic behavior at low stresses such that the corresponding strain is at 0.5% or less [4]. As the stress level increased, deviation from the linearity was found, indicating a nonlinear behavior, which caused difficulty to construct a master curve based on Time-Temperature Superposition principle [5, 6]. Additionally, the time at which the curves start to become nonlinear decreases with the increasing stress levels [7, 8]. Most importantly, the theoretical principles, such as Boltzmann Superposition principle applied in this study, are only valid in the linearly viscoelastic region.

Temperature Effect

It is well known that a change of the temperature has a dramatic effect on the mechanical properties of polymers because a higher molecular mobility is expected at elevated temperatures. Glass transition temperature (T_g), only observed in the polymeric materials, indicates the structural change between glassy and rubbery state. T_g is regarded as a critical reference temperature for assessing mechanical performance of polymers. T_g – 20°C is usually considered as a limiting use temperature for most applications since a significant loss of mechanical performance may occur at this temperature level. Previous findings [6-7, 9] have shown that the tensile modulus of epoxy resin can drop drastically when temperatures approach T_g. These results suggest that the viscoelastic responses of materials essentially become highly nonlinear when the temperature is close to T_g and the service temperature of epoxy adhesives should be strictly limited by this transition temperature.

Moisture Effect

The effect of water in an epoxy resin system has been extensively investigated during the past two decades. Moisture absorption is an unavoidable phenomenon for most epoxy structural adhesives during service because there is a relatively strong affinity with water molecules due to the creation of polar hydroxyl groups from the epoxide ring-opening reaction to form cross-linked structure shown in Fig. 2.1. Generally, the epoxy-based adhesives are vulnerable to the moisture attack, especially in severe humid environments.

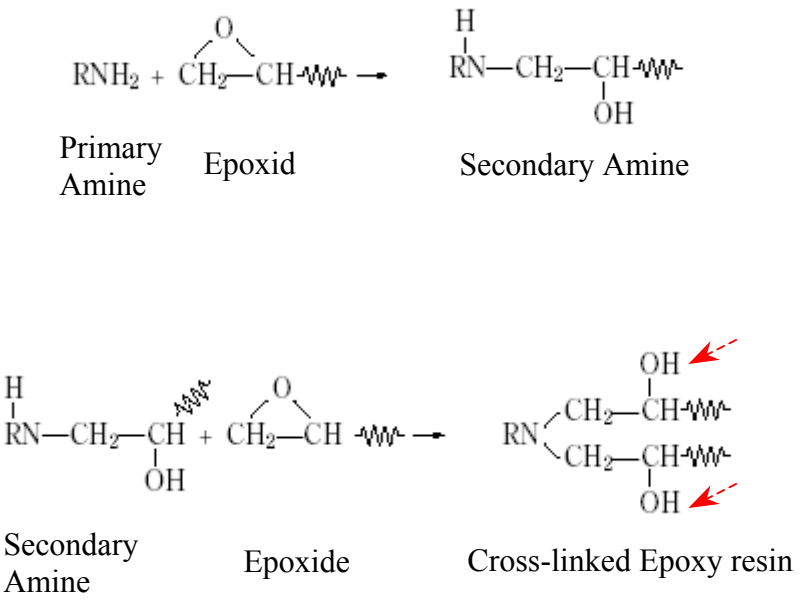

Fig. 2.1. Reaction mechanism of an epoxy-amine curing system; two dashed arrows show the formation of the polar hydroxyl groups in the cured epoxy resin.

Apicella et al. [10] proposed that there are three ways to absorb water for a given epoxy resin: (1) formation of polymer-diluent solution; (2) adsorption at the hydrophilic sites; (3) adsorption on the surface of free volume elements. In terms of the detailed absorption processes, the mechanism of water diffusion has been comprehensively discussed and addressed by the Fick's Second Law [11]. Zhou et al. [12] found that the diffusion coefficients of epoxy resin systems are highly dependent on temperatures; however, the saturated moisture content may be less sensitive to the testing temperatures. Diamant et al. [13] have demonstrated that four main factors have critical influences on the coefficient of moisture diffusion into epoxy resins: the

polymer network structure, the polymer polarity, the physical morphology, and the development of micro-damages. Also, the non-Fick's behaviors of water diffusion have also been reported in neat epoxy resin systems [14]. Due to the cracks, voids, and dissolution, each of these factors may contribute to the deviations of moisture absorption behaviors from the theoretical Fick's diffusion curve [15].

The ATR-FTIR technique has been used as a non-destructive method to characterize the hydrogen bond interactions between water and epoxy resin. Li et al. [16] successfully used this technique to show the quantitative moisture contents in BMI resins. However, the epoxy resin with moisture contents in the matrix can not show a similar quantitative change [17]. One of the reasons is the existing -OH bonds in the cured epoxy systems have overlapped the effect of the absorbed moisture in the same wavelength region (3700-3100 cm^{-1}).

Plasticization and alteration of the T_g are the phenomena often linked to moisture absorption, leading to the change of the mechanical and thermal properties. Typically, the absorbed water can cause harmful effects on the physical properties of the epoxy matrix and greatly compromise the performance of the epoxy-based structural adhesives, such as reductions in tensile modulus and yield strength [18-20]. Besides, suppression of T_g due to moisture uptake decreases the onset temperature for long-chain mobility [21], leading to a drop in the operation temperature of epoxy adhesives.

Moreover, the particle-filled epoxy-based structural adhesives, as the case for the commercial adhesive studied here, can exhibit a more complex non-Fick's behavior

[17, 22]. Usually, the silane-treated glass beads are used in the glass bead-epoxy adhesive as a commercial adhesive and the chemical bonds between the silane and the glass beads may reduce the number of the hydrophilic sites in the interface and the amount of water uptake. [22]. Woo and Piggot [23] has proposed that water in certain epoxy systems is not bonded to any polar groups or hydrogen-bonding sites. Clearly, the interactions between absorbed water and epoxy resins may not be similar for different systems, which imply that the complexity of the diffusion mechanism and moisture effect on epoxy resin systems cannot be generalized without substantiation.

Models for Viscoelastic Behaviors

The time-temperature superposition principle, which involves the reduced time concept, has been extensively utilized for the interpretation of viscoelastic performances [5-9, 24]. Based on the assumption of thermo-rheological simplicity, the short-term experimental data can be shifted individually to construct a master curve at a reference temperature in the linearly viscoelastic range. The temperature dependence of the shift factors can be interpreted as an Arrhenius-type of behavior below T_g for amorphous as well as crosslink systems [6, 9, 24-25].

In the open literature, many empirical models have been applied to describe and predict the long-term viscoelastic behaviors of polymeric materials. The power-law model has been applied to study the viscoelastic behavior of polymers, especially in a short-time period. Mckenna et al. [26] have shown that the power-law relation works over a limited time span for the viscoelastic relaxation of cross-linked networks.

Furthermore, the empirical power-law model seems to fit well only for short-term data [6, 27] since the unlimited retardation spectra from the power-law model cannot describe the entanglement plateau regime found in epoxy resin at longer times. Augl [28] included the longer-time viscoelastic region by adding an additional term to the power-law equation; however, his approach is a purely-empirical adjustment.

Another frequently-applied viscoelastic model is based on mechanical analogues of using springs and dashpots, regarded as Maxwell or Kelvin-Voigt model [29, 30]. A combination of series of the two basic models has been found to fit the experimental creep data adequately, even for complicated composite materials [31, 32]. Generally, the more the elements are incorporated in the viscoelastic model, the higher the accuracy the model can describe the creep behavior. However, the parameters included in these models are purely empirical [27]. That is, this type of viscoelastic model is unable to bear any physical meaning to viscoelastic behaviors of polymers.

The well-known Kohlrausch-Williams-Watts (KWW) form [33, 34], another commonly applied model, can successfully describe the viscoelastic behavior of polymers using a fractional exponential decay function. O'Connell et al. [9] showed that the KWW form can interpret easily the relaxation behaviors of bisphenol A polycarbonate. Furthermore, the viscoelastic mechanical properties of several neat epoxy resin systems can be captured properly using this relationship shown by O'Brien et al. [8]. Raghavan et al. [5] used the same type of stretched exponential relationship to model the creep phenomena of epoxy composites effectively. However, the

fractional exponential parameter that relates to the breadth of spectra still lacks its physical meaning despite its ability to fit the experimental data quite well.

In this study, the Coupling model introduced almost two decades ago by K. L. Ngai [35, 36] is utilized to analyze the creep phenomena of epoxy adhesives. An important attribute of the Coupling model is its ability to physically describe the characteristics of the molecular mobility using a coupling parameter, *n*, and an apparent relaxation time constant, τ^*. The coupling interaction between the molecules and its environment is determined by the Coupling parameter, *n*, as a stretched exponential decay function. Based on this physical interpretation, the Coupling model can be regarded as a predictive model. Another important characteristic of the Coupling model is to preserve the continuity from the primitive exponential function smoothly to the empirical KWW function in the entire scale of time. When *n* is equal to zero then the Coupling equation describes a simple exponential decay as imagined as the Debye relaxation phenomenon. When *n* value increases, then the breadth of the relaxation distribution also increases, indicating the increased level of the coupling cooperation with the surroundings. The details of the Coupling Model can be referred to the published literature [37-39]. In term of material structural state, the Coupling parameter reflects the level of constraint for molecular species to relax in a given surrounding environment [40]. Roland et al. [41] showed the evidence that an increase in intermolecular constraints associated with higher crosslink density results in a larger Coupling parameter, *n*. Given the uniqueness of the physics-based model, the

Coupling model can be regarded as a fundamental and derivable model for describing the viscoelastic behavior of polymers.

Viscoelastic Behaviors with Environmental Coupled Effects

Since the coupled actions of load and moisture attack give rise to a complex phenomenon of viscoelastic properties, only limited literature can be found that address the viscoelastic behaviors of polymers with combined load and moisture effects. The modeling of moisture effects on the mechanical behavior of polymers remains an open issue, even when the hydrothermal conditions are only restricted to physical interactions. Time-humidity superposition has been applied to extrapolate long-term performance using several short-term creep data at different relative humidity levels [42]. However, arbitrary correction factors are required to generate a smooth master curve and compensate for the nonlinear creep responses. Wang et al. [22] pointed out that the time-temperature-moisture superposition may not be applicable to construct the master curve of the glass bead-epoxy composites. It has also been found recently [43] that the time-temperature-moisture superposition is inadequate for the long-term prediction of polymer creep behavior since temperature and moisture can not be considered as an isolated factor that affects the viscoelastic behaviors independently.

Other studies focus on the creep behavior of polymers that have already possessed a saturated level of moisture content. The experimental results have shown that the absorbed water not only can lower the T_g of the matrix but also leads to plasticization of the epoxy matrix [6]. An attempt was made to quantitatively establish

the equivalence between temperatures and the presences of moisture on the creep behavior of epoxy composites. Nevertheless, the loss of the water from the wet plain matrix during the tests, especially at elevated temperature, are reported in both cases [6, 22], resulting in inability to construct master curves.

Summary

In order to predict the viscoelastic behaviors of epoxy adhesives, it is necessary to take each relevant effect into account, such as applied stress, moisture, and temperature. Especially, with the coupled effects of moisture absorption, the complexity of the creep phenomenon may be raised dramatically. How to evaluate the long-term performance of structural adhesives under different conditions in a short period of time is the potential target based on the previous study. A designed accelerated immersion test to study the moisture effect on the creep behavior is proposed in the following chapter, and the Coupling model is utilized to analyze the creep phenomena of epoxy adhesives under different environmental conditions.

CHAPTER III

THEORETICAL CONSIDERATIONS

This chapter mainly describes the theories and models used in this research. The first section describes the diffusion mechanism of water through a material. The second section describes a theoretical formulation for estimating the glass transition temperature of a polymer-diluent system. The third section describes the time-temperature superposition principle. The fourth section entails the viscoelastic behaviors in the linear region. The fifth section validates the relationship between modulus and compliance based on the Boltzmann Superposition. The last one provides details for the Coupling model and how to utilize this predictive model.

Moisture Diffusion Model

The diffusion coefficients are calculated from the moisture uptake profiles based on Fick's second law of diffusion [11]

$$\frac{\partial c(x,t)}{\partial t} = D\frac{\partial^2 c(x,t)}{\partial x^2} \tag{3.1}$$

where *c(x,t)* is the moisture concentration, *t* is diffusion time, *D* is diffusion coefficient, and *x* is distance along space axis.

The Fick's law holds true for the conditions of an infinite sheet with a constant penetration activity on both sides of the sheet and a concentration-independent diffusion rate. The diffusion coefficients are calculated from the moisture uptake profiles:

$$\frac{M_t}{M_s} = 4\left(\frac{Dt}{h^2}\right)^{1/2}\left[\frac{1}{\pi^{1/2}} + 2\sum_{n=0}^{\infty}(-1)^n \, ierfc\frac{nh}{2(Dt)^{1/2}}\right] \tag{3.2}$$

where M_t is the moisture uptake at time t; M_s is the equilibrium saturation moisture content; h is the sample thickness.

At a very short time and when $\frac{M_t}{M_s}$ is less than 0.5, the relationship can be approximated as follows:

$$\frac{M_t}{M_s} = \frac{4}{h}\left[\sqrt{\frac{D \cdot t}{\pi}}\right] \tag{3.3}$$

The Fick's curve profile can be also generated through a simple relationship developed by Shen and Springer [18]:

$$\frac{M_t}{M_s} = 1 - \exp\left[-7.3 \cdot \left(\frac{Dt}{h^2}\right)^{0.75}\right] \tag{3.4}$$

The diffusivity and the saturation moisture level for each system can be obtained by curve-fitting the experimental moisture uptake data.

Fox Equation

The glass transition temperature of the polymer-moisture system can be estimated based on the polymer miscibility theory [3]. This relationship can be applied to plasticizers, i.e., a low-molecular-weight compound (such as water) dissolved in the polymer matrix. The Fox equation derived from this relationship follows

$$\frac{1}{T_g^f} = \frac{W_m}{T_g^m} + \frac{W_w}{T_g^w} \tag{3.5}$$

where T_g^f is the final-state glass transition temperature; T_g^m and T_g^w (-150°C) are the glass transition temperature of the polymer matrix and water. W_m and W_w are the weight fractions of the matrix and water. The temperature is expressed by an absolute temperature unit in this relationship.

The polymer-diluent relationship as represented by Fox equation (3.5) is shown in Fig. 3.1, which is a plot of T_g of the moisture-plasticized epoxy matrix as a function of epoxy weight fraction. Due to the low T_g of water, the effect is the lowering of the glass transition temperature of epoxy. A secondary effect is the lowering of the epoxy modulus, softening it through much of the temperature range of interest.

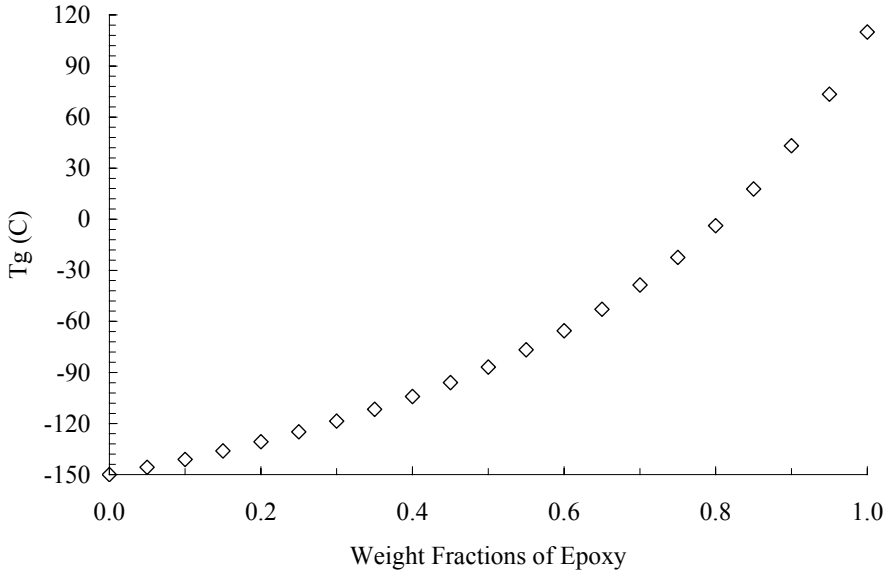

Fig. 3.1. T_g of the epoxy-moisture complex according to Fox equation.

Time-Temperature Superposition

The creep behaviors occur by molecular diffusional motions which become more rapid when the test temperature is increased. The well-established time-temperature superposition principle states quantitatively [44] that for viscoelastic materials, time and temperature are equivalent to the extent that data at one temperature can be superimposed on data at another temperature by shifting the curves along the time scale as shown in Fig. 3.2.

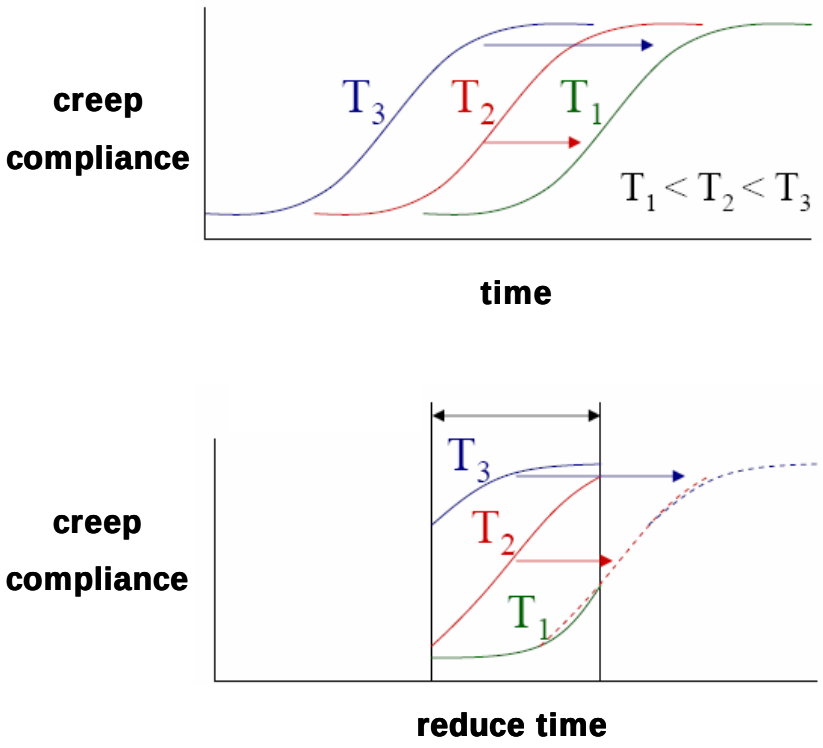

Fig. 3.2. Time-temperature superposition and the formation of a master curve (both X and Y axes are in a log scale).

By recording the time shift required to form the master curve, a shift factor, A, has an Arrhenius relationship below T_g [2]

$$A = A_0 \exp(\frac{E_a}{RT}) \tag{3.6}$$

where A is the shift factor; A_0 is a constant; E_a is the apparent activation energy; T is a testing temperature by an absolute temperature unit, and R is Boltzmann constant.

Linear Viscoelasticity

A time-dependent material behavior is referred as a property of viscoelasticity. A constant load, σ_1, is applied to a viscoelastic specimen and the time-dependent strain is recorded as ε_1; another larger load, σ_2, is applied and the time-dependent strain is recorded as ε_2. If at a particular time t_1 and t_2 after loading, ε_1 and ε_2 are linear with the magnitude of corresponding stress, σ_1 and σ_2, the stress-strain relationship can be given as following

$$\varepsilon_1(t_1)/\sigma_1 = \varepsilon_2(t_1)/\sigma_2 = D(t_1) \tag{3.7}$$

$$\varepsilon_1(t_2)/\sigma_1 = \varepsilon_2(t_2)/\sigma_2 = D(t_2) \tag{3.8}$$

where $D(t)$ is the creep compliance referred as the ratio of strain to stress.

This property is often characterized as linear viscoelasticity. In the linearly viscoelastic region, the creep strain at any given time is a linear function of stress. That is, the creep compliance is independent of stress magnitude, i.e., the creep compliance can be described as a function of time and temperature only, at any applied load (Fig. 3.3).

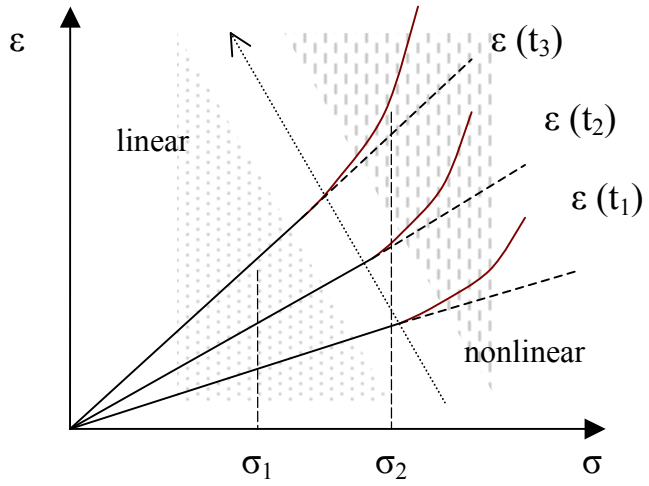

Fig. 3.3. The Linear-nonlinear transition region of stress-strain relationship with respect to different time levels.

The supposed transition from a linear to a nonlinear behavior would be the evident by the deviation from the slopes of creep compliance curves with increasing stresses. These linearity checks were made at the lowest and highest test temperatures for each set of creep experiment thereby to stay in the linearly viscoelastic region. In Fig. 3.4, the applied stress, which can generate 0.6% strain, shows the dependence on both time and stress for the model epoxy system at 22°C. Conversely, the strain below 0.4%, applied as an initial strain, can generate the linearly viscoelastic responses. Hence, the 0.3% strain, chosen as the initial strain for the creep experiments can maintain in the linearly viscoelastic region. Since the polymers may tend to behave as

nonlinearly viscoelastic materials due to high molecular mobility, the isochronous tests were also performed at the highest testing temperature (67°C) to confirm that creep test with a 0.3% initial strain in this temperature range stays in the linearly viscoelastic region in Fig. 3.5.

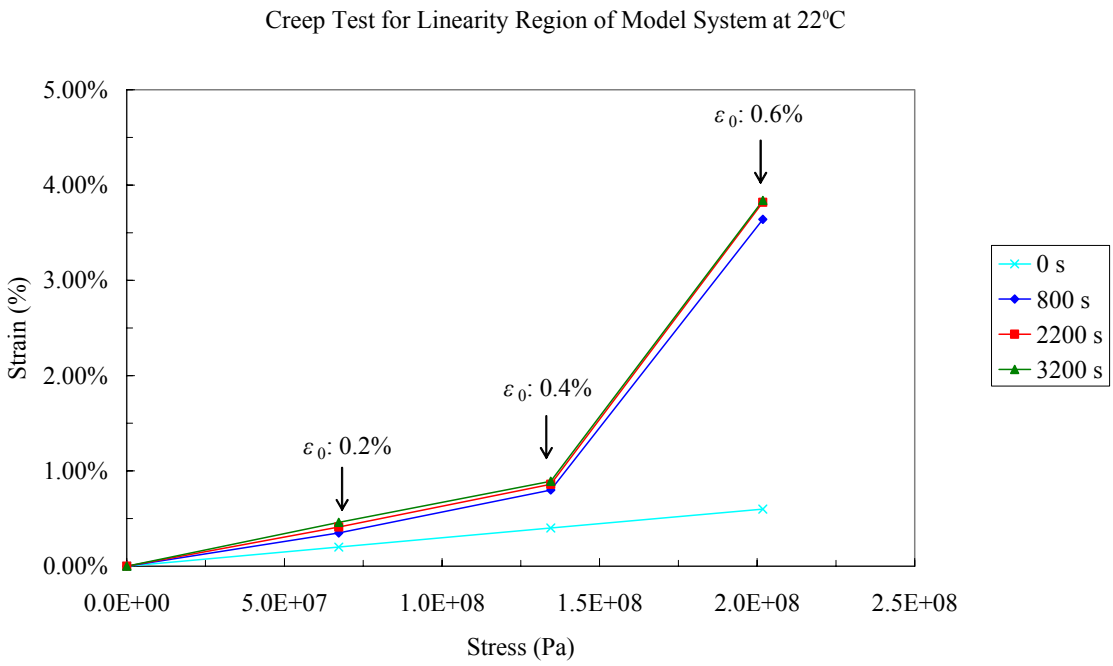

Fig. 3.4. Creep test at 22°C with loads generating initial strain 0.2%, 0.4% and 0.6%.

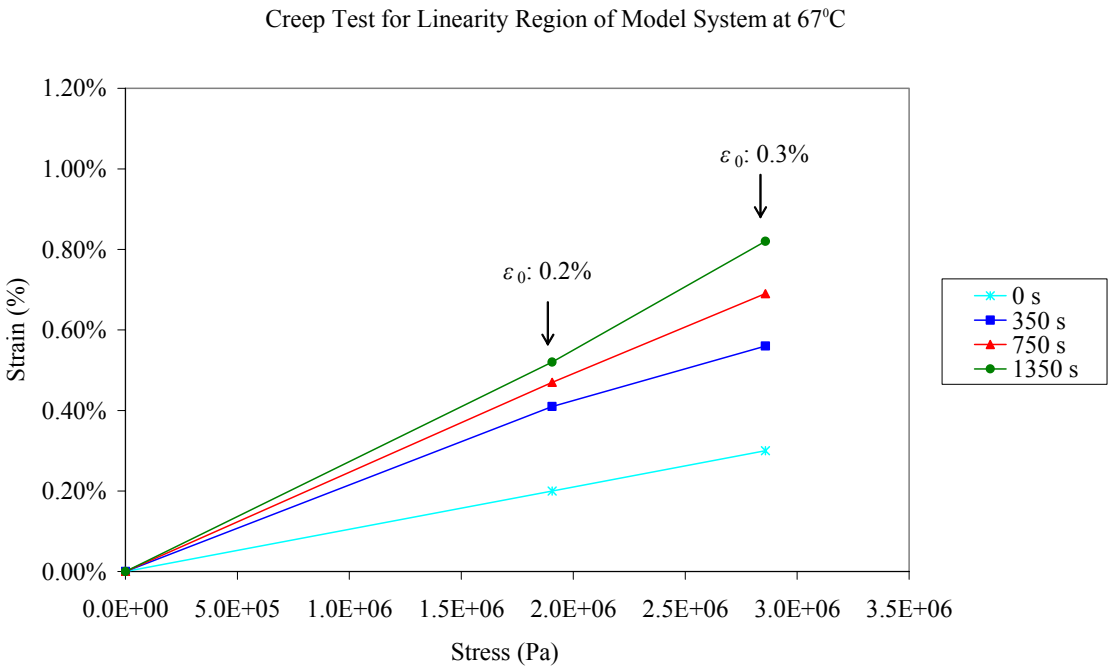

Fig. 3.5. Creep test at 67°C with loads generating initial strain 0.2% and 0.3%.

Boltzmann Superposition

The Boltzmann Superposition principle plays a central role in the representation of linearly viscoelastic behavior [2, 39], where the response of a material under a given load is independent of the response of the material to any load which has previously been applied to that material. The deformation of a specimen is directly proportional to the applied stress when all deformations are compared to equivalent times. It assumed that in the linearly viscoelastic region the stress and strain relationship follows

$$\varepsilon(t) = \int_0^t D(t-\tau)\left(\frac{d\sigma}{dt}\right)_{t=\tau} d\tau \tag{3.9}$$

$$\sigma(t) = \int_0^t E(t-\tau)\left(\frac{d\varepsilon}{dt}\right)_{t=\tau} d\tau \tag{3.10}$$

where $D(t-\tau)$ and $E(t-\tau)$ is the creep compliance function and the stress-relaxation modulus, respectively.

The two functions can, however, be related *via* the Laplace transforms to convert the constitutive equations which follow the Boltzmann integrals

$$\int_0^t D(t-\tau)E(\tau)d\tau = \int_0^t E(t-\tau)D(\tau)d\tau = t \tag{3.11}$$

The explicit relationship between $E(t)$ and $D(t)$ can be expressed by

$$D(t) = \frac{\sin(m\pi)}{m\pi} \cdot \frac{1}{E(t)} \tag{3.12}$$

where m is the slope of the creep compliance curve as a function of time in log scale.

Fig. 3.2 shows several creep compliance curves and a superimposed master curve. As time approaches to zero or infinity, the slope, m, become zero. For these two extreme boundary conditions, the equation (3.12) can be approximated by the L'Hopital's Rule:

$$\lim_{m\to 0} \frac{\sin(m\pi)}{m\pi} = \frac{\pi \cdot \cos(m\pi)}{\pi} = \cos(m\pi) = 1 \tag{3.13}$$

$$D(t) = \frac{1}{E(t)} \text{ ; } \textit{only} \text{ when } t \to 0 \text{ or } t \to \infty \tag{3.14}$$

It is important to note that the compliance is the reciprocal of the modulus for a perfectly elastic solid. For the viscoelastic materials, however, the relationship is only valid when time approaches to zero and infinity as dedicated above.

Coupling Model

The Coupling model proposed by Ngai almost two decades ago [35,36] has remained unmodified and been considered as a predictive model. Here, the relaxation relationship is used to explain the Coupling model. The relaxation quantity *Q(t)* obeys a simple rate equation with a constant relaxation rate in the primitive relaxation mode, where the coupled effect to its complex environment is not yet considered.

$$\frac{\partial Q(t)}{\partial t} = -\frac{Q(t)}{\tau_0},\ t << t_c \tag{3.15}$$

$$\frac{\partial Q(t)}{\partial t} = -\frac{Q(t)}{\tau_0}(\omega_c t)^{-n},\ t >> t_c \tag{3.16}$$

where τ_o is primitive relaxation time, t_c is a temperature insensitive crossover time, $\omega_c \equiv t_c^{-1}$, n is the coupling parameter whose value lies within the range $0 \le n \le 1$ and depends on the intermolecular interaction.

$$Q(t) = Q(0) \cdot \varphi(t) \tag{3.17}$$

where $Q(0)$ is the initial relaxed quantity and $\varphi(t)$ is the relaxation correlation function.

$$\varphi(t) = \exp\left(-\frac{t}{\tau_0}\right),\ t << t_c \tag{3.18}$$

$$\varphi(t) = \exp\left(-\frac{t}{\tau^*}\right)^{1-n},\ t >> t_c \tag{3.19}$$

For polymers, such a cross-over can be observed by neutron scattering methods for segmental motions. The continuity of the molecular motion from Debye relaxation

to segmental motions can link these two equations (3.18 and 3.19) when time is equal to the crossover time

$$\tau^* \equiv [t_c{}^{-n}\tau_0]^{1/(1-n)}; \text{ when } t = t_c \tag{3.20}$$

For very weak coupling, n is nearly zero and the factor, $(\omega_c t)^{-n} \cong 1$ so there is little modification of the rates. Conversely, for stronger coupling, n takes larger values leading to a slower relaxation rate. The coupling value, n, can be regarded as a physical parameter to evaluate the segmental molecular constraints. The relaxation kernel can be also implemented into the creep equation [41]

$$D(t) = D_0 + (D_e - D_0) \cdot (1 - \exp[-(t/\tau^*)^{1-n}]) \tag{3.21}$$

where D(t) is the creep compliance as function of time, D_0 and D_e are the initial compliance and the equilibrium compliance respectively.

Here, a detail how to derive the two crucial parameters, D_0 and D_e is addressed. In the linearly viscoelastic region, the creep compliance, $D(t)$, mainly depends on time (t) and temperature (T) in the form

$$D(t) = \frac{\varepsilon(t,T)}{\sigma_0} \tag{3.22}$$

where $\varepsilon(t, T)$ is the strain as a function of time and temperature; σ_0 is the initial stress.

Based on the relationship derived from the Boltzmann Superposition in the previous section, the initial compliance, D_0, can be estimated as

$$D_0 = \frac{1}{E_0}; \text{ when } t \to 0 \tag{3.23}$$

where E_0 is the modulus when time approaches to zero. The E_0 can also be equated to the elastic modulus obtained by a tensile test.

The value of shear modulus, G, from DMA result can be represented by the storage modulus, G', and loss modulus, G", in complex form

$$G = G' + iG'' \tag{3.24}$$

In the rubbery plateau stage, at which the ratio of loss and storage modulus is only about 2%~4%, it means the loss modulus can be neglected and the complex modulus is approximately equal to the storage modulus in this stage. Hence the equilibrium modulus can be derived from the rubber plateau modulus, G_r [45]

$$E_e = G_r \cdot 2(1+\nu) \tag{3.25}$$

As for the equilibrium compliance, D_e,

$$D_e = \frac{1}{E_e}; \text{ when } t \to \infty \tag{3.26}$$

where E_e is converted from G_r by the Poisson ratio, υ, which is equal to 0.5 since the epoxy resin material is in the rubber state.

CHAPTER IV

EXPERIMENTAL WORK

Materials

Two sets of epoxy systems were chosen for this study. One is a simple model epoxy resin (model epoxy system). The other is a complex commercial structural epoxy adhesive (commercial epoxy system). The details of the material description are listed in Table 4-1.

Table 4-1 Material list of the model and commercial epoxy resin systems.

Model Epoxy Resin System	
DER® 331	Dow Chemical; *EEW**: 182-192
DER® 732	Dow Chemical; *EEW**: 305-335
Versamid® 140	Cognis Corporation; *HEW***: 97
Commercial Product System	
BETAMATE™ 73316/73317	Dow Automotive

*Epoxide Equivalent Weight; **Hydrogen Equivalent Weight.

The model epoxy system is composed of diglycidyl ether of bisphenol A (DGEBA) epoxy and a polyamide (Polyaminoimidazolin) curing agent mixed at a stoichiometric ratio of 2:1 by weight, along with a high molecular weight flexibilizer, i.e., DER 732 (polyglycol diepoxides), at 5% equivalent weight to increase flexibility and processibility. The reaction of polyamides with epoxy resin is similar to that of the aliphatic amines. However, since the polyamides are relatively large polymers, the ratio

of polyamide to epoxy is less critical than with the low-molecular-weight amines. The chemical structure of DGEBA has been shown in Fig. 4.1. The commercial epoxy system is a two-component adhesive system widely used in bonding aluminum substrates for structural applications. Fig. 4.2 illustrates a fracture surface of the commercial adhesive, showing the complex matrix with highly loading of hollow glass beads (D: 50μm).

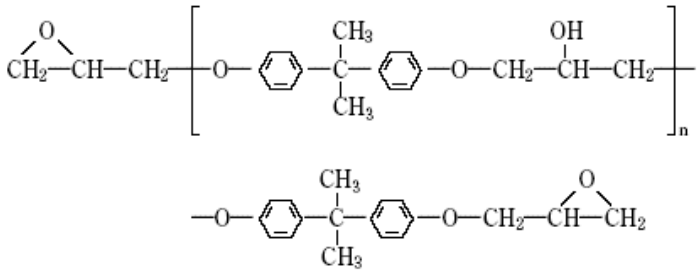

Fig. 4.1. Diglycidyl ether bisphenol A epoxy resin (DER® 331).

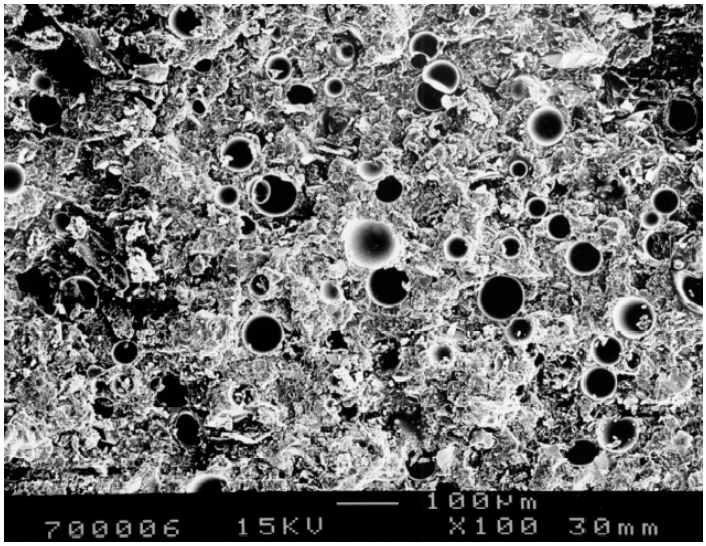

Fig. 4.2. A SEM picture of the commercial epoxy adhesive.

The model epoxy system is a base formulation of the commercial epoxy adhesive system, which can be regarded as a reference epoxy system. The curing schedule for each system is 50°C for one hour and 120°C for three hours, followed by cooling in an oven overnight. The curing schedule to reach fully cured state was determined using differential scanning calorimeter (DSC) isothermal tests. Attenuated-total-reflectance FTIR (ATR-FTIR) spectroscopy analysis was also performed to determine the extent of curing.

Differential Scanning Calorimetry (DSC) Test

An isothermal DSC test (Perkin-Elmer Pyris-1) was performed on both systems to characterize the curing process. The whole curing schedule was monitored for three hours at 120°C in nitrogen gas environment. The curing schedule was determined by conducting isothermal tests in order to reach fully cured cross-linked network structure.

Tensile Test

The tensile tests were conducted in accordance to ASTM Standard D638 (Specimen Type IV) using the Sintech-II Mechanical Test System. The engineering moduli were investigated at different temperatures under both dry and the corresponding saturated moisture conditions. The tensile test was performed at a strain rate of 2”/min, and the tensile strain was obtained using an MTS extensometer attached to the samples. The temperature the specimen experiences, which was controlled using

the OMEGA CN76000 temperature controller in an environmental chamber, was monitored using a thermocouple located at about 2 mm away from the samples.

Moisture Diffusion Test

The dimensions of samples for moisture absorption studies are 25mm x 25mm x 1.5mm (length x width x thickness). The specimens were machined from the cured flat panels and stored in vacuum desiccators for at least three days until a constant weight was achieved. They were put into a humid environment at 22, 31, 40 and 49°C, respectively, in a Blue M Convention Oven and exposed to 95% relative humidity (R.H.) air, which is achieved by suspending specimens above water in sealed glass jars. Specimens were taken out periodically to monitor their weights using an analytical balance with a precision of $\pm$ 10^{-5}g until the weight reaches equilibration. The weight gain percentage, M_t, can be determined from the following equation:

$$M_t(\%) = \frac{(W' - W_0)}{W_0} \times 100\% \tag{4.1}$$

where W' is the weight of water-absorbed epoxy specimen, and W_0 is the initial weight of the dry specimen. Before the samples were weighed, they were kept in a sealed beaker with 95% R.H. at ambient temperature for 5 minutes in order to allow the samples to cool down. Care was taken to wipe off any extra water on the specimen surfaces. The time for weight measurement was subtracted from the calculated exposure time. Eventually, the weight gain measurements were continued until the weight gain reached a plateau value, which signifies the moisture saturation state.

Water Immersion Test

Water immersion test was performed in order to reach saturation moisture level in a much shorter time. The model and commercial systems were put into deionized water at 40°C for 4 days and 58°C for 3 days in Blue-M Conventional Ovens, respectively. The immersion duration times and the moisture saturation levels were chosen based on the moisture diffusion tests. The weight gain measurements were taken in a similar manner as mentioned in the previous section.

Another set of experiments was designed to monitor possible water losses of these two moisture saturated epoxy systems in humid environment. After the immersion tests, the moisture saturated samples of the model system were put into 95% R.H. condition at 22°C and 49°C, individually; the moisture saturated samples of the commercial system were put into 95% R.H. condition at 22°C and 40°C, correspondingly. The moisture contents after one day were compared with the existing contents to confirm the validity of the accelerated moisture uptake experiments. The condition at which the sample is in the saturated moisture level would be regarded as the "wet" condition.

Fourier Transform Infrared (FTIR) Test

Attenuated-total-reflectance FTIR (ATR-FTIR) spectroscopy analysis was performed on epoxy sample surfaces using Nicolet Avatar 360 System with a resolution of 8 cm^{-1}. The wave-numbers scanned range from 750-3500 cm^{-1}. FTIR was used to monitor the extent of cure for the model and commercial epoxy systems.

ATR-FTIR tests were also conducted during the immersion process and the sample handling method is the same as those prepared for measuring moisture saturation. This technique can simultaneously monitor any possible unexpected reactions that might take place during the water immersion tests.

Dynamic Mechanical Analysis (DMA)

DMA tests (Rheometrics RMS-800) were performed on both model and commercial epoxy systems in a torsion mode, with 5°C per step and at 1 Hz frequency. Strain sweep tests were first conducted at strain range from 0.01% to 0.5% to determine the linearly viscoelastic region. A 0.1% and 0.15% sinusoidal strains were chosen for model and commercial epoxy system, respectively, to ensure that the epoxy samples behave within the linearly viscoelastic region. The samples in the dry and wet conditions were tested individually at temperatures ranging from -90°C to 160°C. The transition temperatures at which the highest localized tangent delta peak values (tan (δ)) located are assigned as α-transition (T_g) and β-transition (T_β) temperatures. The temperature sweep tests at frequencies 0.1, 1, and 10Hz were performed to determine the activation energies for both epoxy systems.

Creep Test

A custom-built creep station, shown in Fig. 4.3(a), was employed to carry out the creep tests. A constant load was imposed on the specimens by means of a pneumatic cylinder (Motion Controls, D series; push power factor: 1.23) and a constant

temperature was controlled (by OMEGA® CN76000 Controller) in the environmental chamber with thermocouples (OMEGA® J-Type). The mercury thermometer with sensitivity of 0.1°C was applied to calibrate the thermocouple at ambient temperature for each creep experiment. The vertical displacement, which was measured using LVDT sensor (Solartron Mach1 series) with 10^{-3} inch sensitivity and the corresponding time were automatically recorded using LabView® software. The dimensions of the creep test specimens are 100mm x 15mm x 1.5mm, as shown in Fig. 4.3(b). A hole was drilled on each end of the sample and a spacer was attached to prevent slip and to increase the stiffness near the grip region of the specimen. The gage length was determined by the distance between two spacers for each sample. The slippage and local stress-concentration near the grip can be prevented by the pins of clamps and the spacers, respectively.

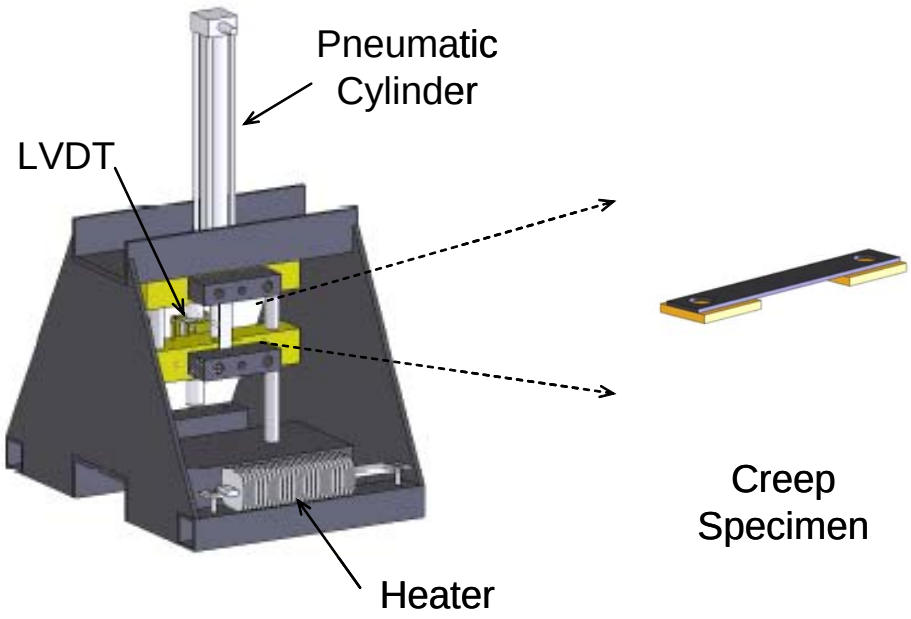

Fig. 4.3. The illustrations of (a) the creep station, and (b) the creep specimen.

The dry and wet specimens were tested at different temperatures in the dry and 95% R.H. wet environments. The highest test temperature for the dry conditions was determined by the temperature at which the tensile modulus drops to half of its corresponding value at room temperature since the viscoelastic response of epoxy also becomes highly nonlinear when the test temperature is close to T_g. Normally, polymeric materials exhibit linearly viscoelastic behavior at low stresses such that the corresponding strains are at 0.5% or less [4]. The determination of the stress level in the linearly viscoelastic region was made by conducting a series of isochronous creep tests at the lowest and the highest test temperatures, which have been shown in Fig. 3.4-5. Before starting the test, each test was held for 30 minutes until the equilibrium environmental condition was reached. The repeated creep tests were performed for each condition to ensure reproducibility. The displacement as a function of time can be described as a creep compliance, *D(t)* (1/Pa):

$$D(t) = \frac{\varepsilon(t)}{\sigma_0}; \text{ where } \sigma_0 = \frac{F}{A} \tag{4.2}$$

$$\varepsilon(t) = \frac{\Delta L(t)}{L_0} \tag{4.3}$$

where $\varepsilon(t)$ is the engineering strain as a function of time, F is the applied load and A is the cross-sectional area of the specimen, $\Delta L(t)$ is the displacement as function of time and L_o is the original gauge length.

Additionally, the calibration for the creep station was performed by using a load cell (Wagner Instrument FDL100, Model 301, with precision $\pm$ 0.3%) to check the push factors of the cylinders against those reported by the manufacturer and to verify the

errors between the output loads and the applied air pressure. The linearity and match of the slope between applied pressures and output loads (push factor) are shown in Fig. 4.4. The root-mean square error between the values from the load cell and those calculated from the air pressure is 0.051, and 0.073, respectively, which is satisfactorily small compared with the minimum applied load about 5.0 lb.

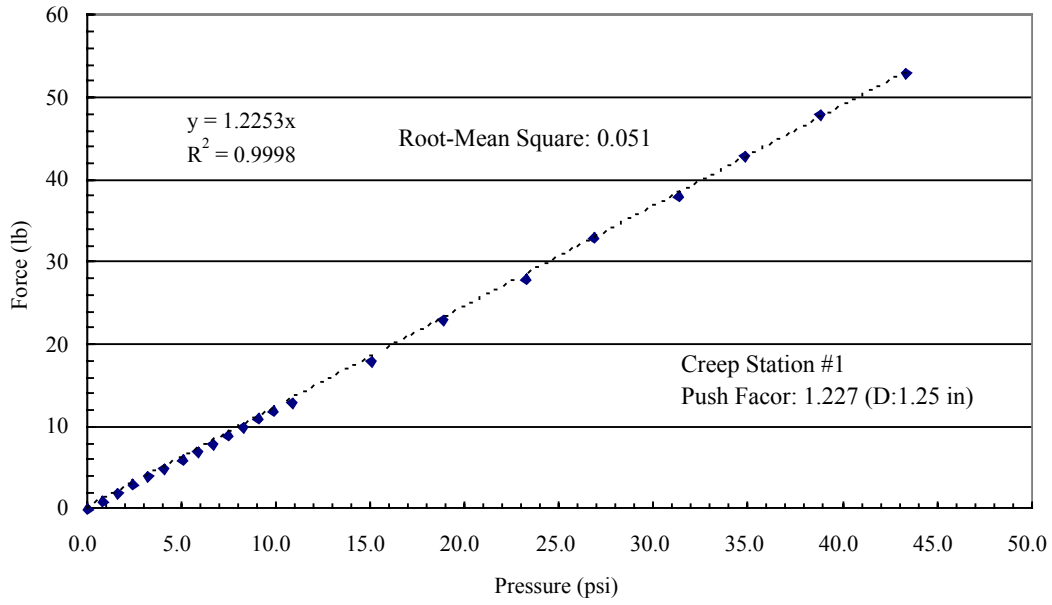

(a)

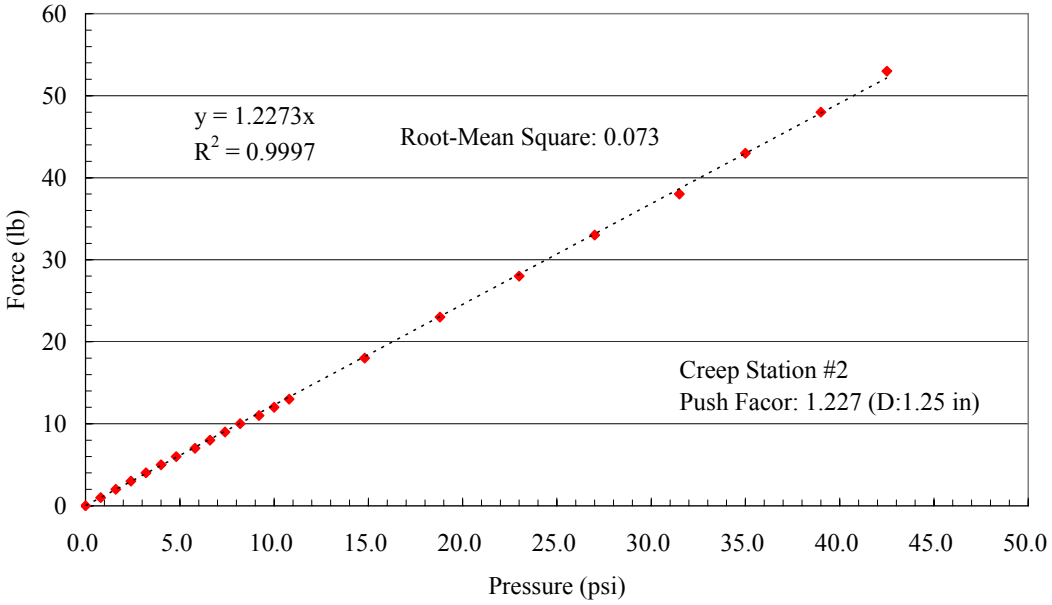

(b)

Fig. 4.4. Calibrations for the (a) creep station #1, and (b) creep station #2.

CHAPTER V

RESULTS AND DISCUSSION

Tensile Test Result

The tensile moduli as a function of temperature for each system are shown in Fig. 5.1. The arrows indicate that the modulus at elevated temperatures drops to its half value of the room temperature value. Those temperatures were chosen as the highest creep test temperatures for each epoxy system in the dry condition to avoid undergoing nonlinearly viscoelastic behavior. It is also the evident that the test temperature has a significant effect on the modulus of the epoxy systems, especially for the commercial epoxy system, which has a rather low T_g. The moduli for the model and commercial epoxies in the wet condition were observed to be 20% to 40% lower than those in the dry condition, respectively, which suggests that moisture exposure indeed deteriorates the mechanical performance significantly even with only a small amount of moisture uptake.

DSC Test Result

Fig. 5.2 shows that the reactions of both systems are complete after 30 minutes at 120°C under DSC isothermal experiments. The flat curve also indicates that there is no further reaction and/or degradation at the curing temperature during testing. Since any further chemical reaction due to incomplete curing may induce analysis complexity, the curing schedule based on the DSC test result can ensure both systems are fully cured.

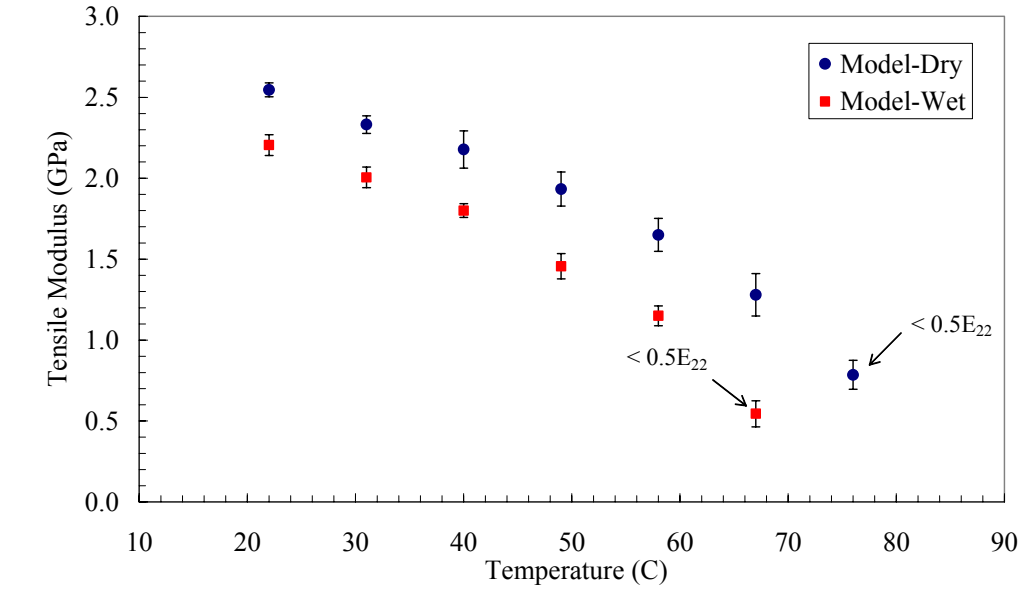

(a)

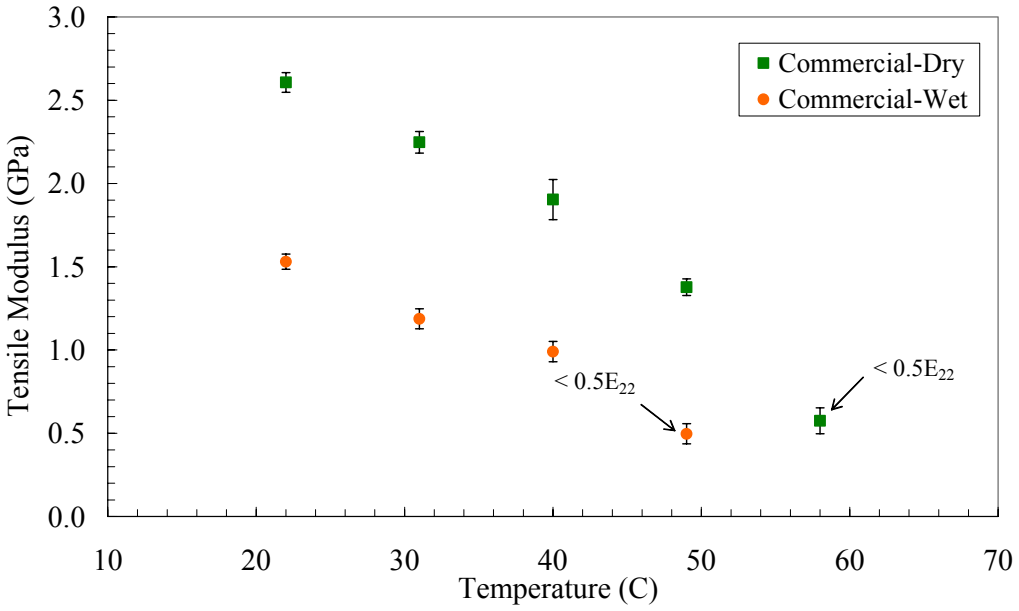

(b)

Fig. 5.1. The tensile moduli of (a) model system; (b) commercial system.

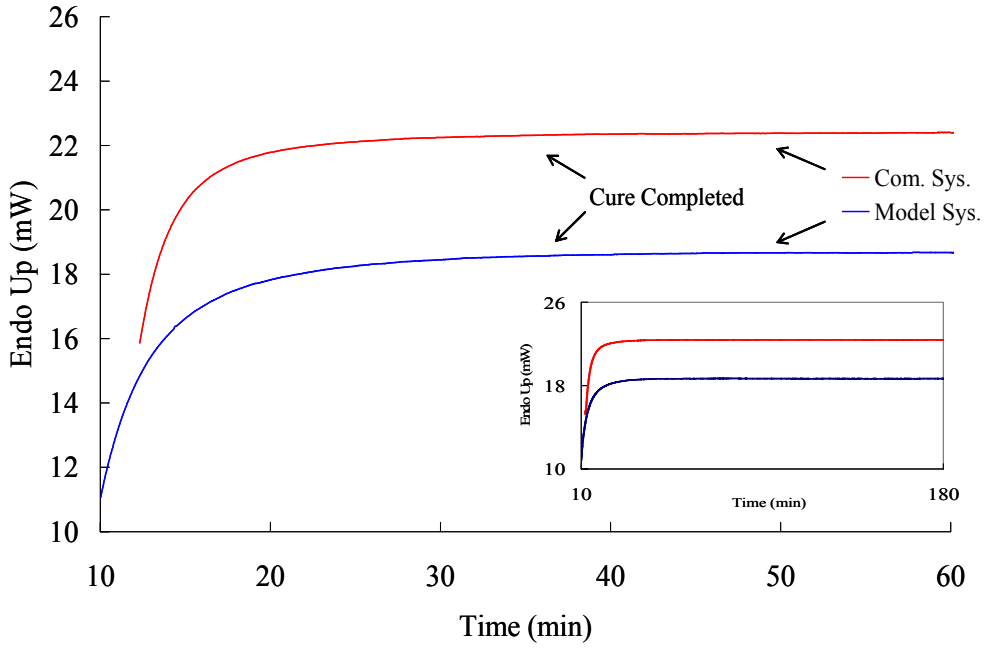

Fig. 5.2. The isothermal DSC tests at 120°C for both epoxy systems.

Moisture Diffusion and Immersion Result

The moisture absorption profiles of the two systems in the 95% R.H. environment for about 150 days at different temperatures are illustrated in Fig. 5.3. The dots are the experimental moisture uptake data. The solid curves are the curves fitted by the Fick's Second Law. The diffusion coefficient was determined by using equation (3.3). The saturated moisture levels for model and commercial epoxy systems are 3.7% and 2.8% by weight, respectively. A similar moisture saturation level (3.5%) was also reported by Nakamura et al [46] using the same DGEBA-polyamides epoxy system.

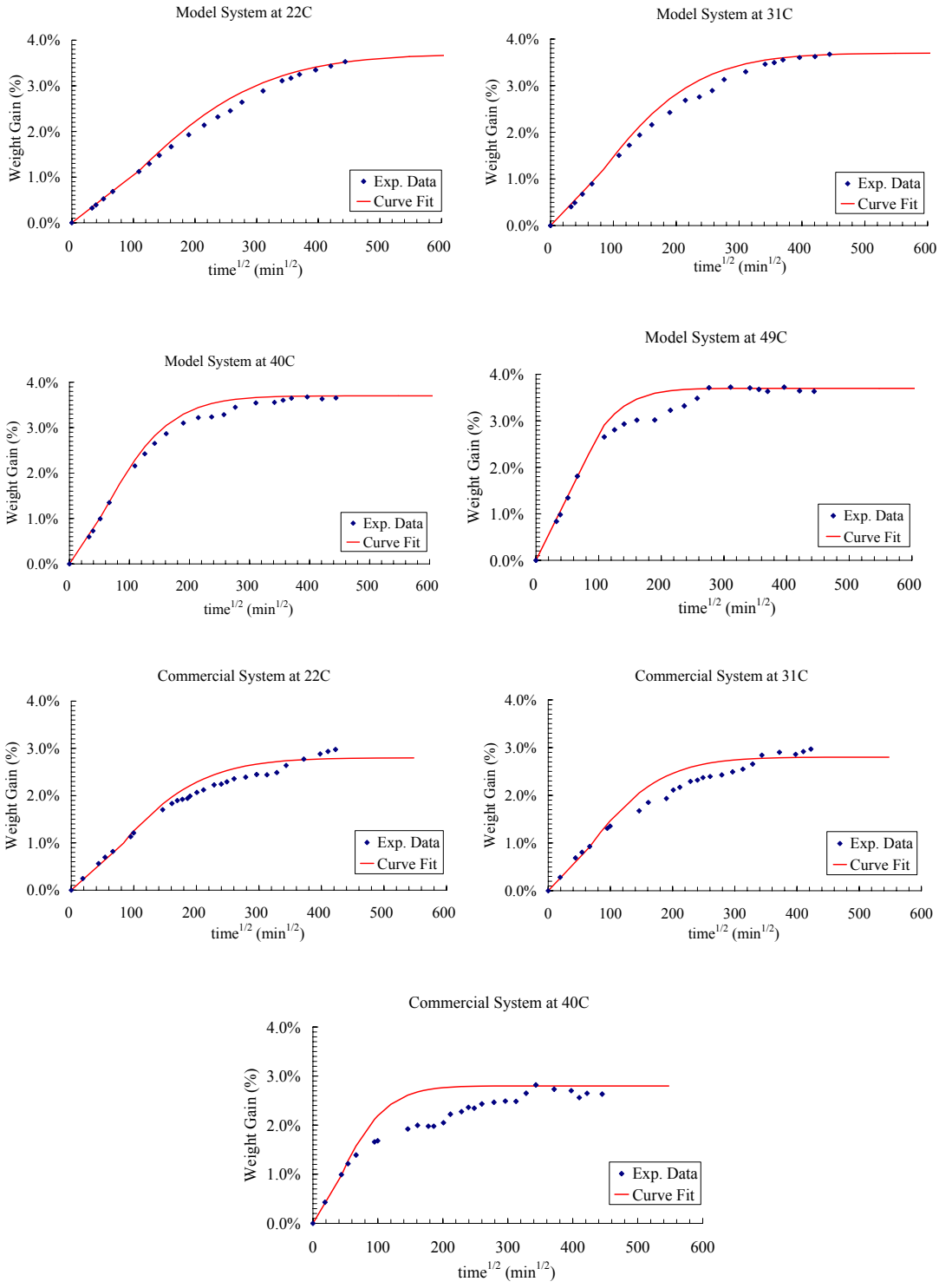

Fig. 5.3. Moisture diffusion profiles and Fick's Law curve fitting.

The diffusion coefficients, D, can also be utilized to obtain the activation energy, E_D for the diffusion process by using an Arrhenius type equation to describe the temperature dependence of the diffusion coefficients, D:

$$D = D_0 \exp(\frac{E_D}{RT}) \tag{5.1}$$

where D_0 is the constant, E_D is the activation energy of moisture diffusion. T is the testing temperature expressed by an absolute temperature unit, and R is the Boltzmann constant. Fig. 5.4 shows this Arrhenius relationship by plotting *log(D)* versus *1/T* and the activation energy for the diffusion process can be derived from the slopes of Arrhenius plots for the model and commercial epoxy systems, respectively.

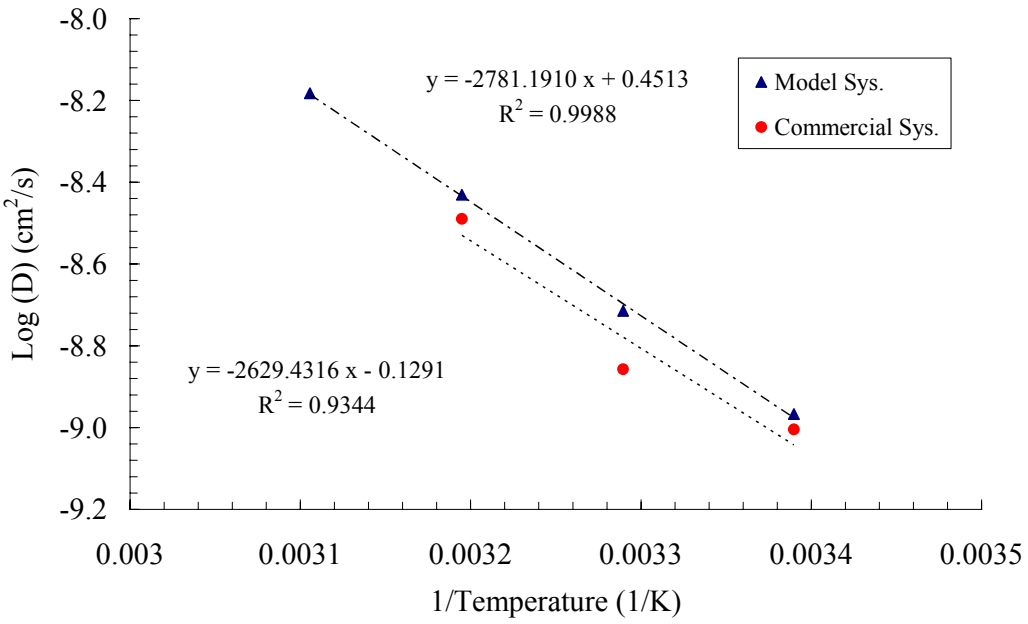

Fig. 5.4. The Arrhenius relationship between diffusion coefficients and temperatures.

The initial moisture absorption is characterized as being a fast process and the percentage of moisture gain is linearly proportional to $time^{1/2}$, based on the equation (3.3). In the initial stage, the rate of uptake will either increase or decrease depending on the direction of temperature change. Most cases, shown in Fig. 5.3, follow the Fick's Second Law in this regime. The deviations from the Fick's behavior are encountered in the intermediate stage of the moisture uptake and even become more pronounced at higher temperatures. The same phenomenon has been observed by Soles *et al.* [14]. One of the possible explanations is the diffusivity being an increasing function of concentration, which brings the linearity to higher M_t/M_s value (>50%). However, the self-adjustment of the moisture diffusion during the intermediate stage may be eliminated once the gradient of the moisture content through the sample becomes smaller (when approaching the equilibrium stage). Then, the moisture content essentially remains unchanged over a long period of time in the final stage. This region may also be related to a "physical/chemical equilibrium" regime. If the epoxy resin matrix or additives allow for chemical interactions with water, then this regime becomes extremely sensitive to aging duration and external factors, such as temperature. The large deviations from the Fick' Law observed at the final stage of the commercial system may be explained by these interactions. Table 5-1 shows the diffusion coefficients of both systems at different temperatures (data of the commercial system at 49°C is not given since it is close to its T_g) and the activation energies for moisture diffusion mechanism. The moisture diffusion coefficients are highly dependent on the surrounding temperatures. The lower diffusion coefficients and saturated moisture

level suggests that there may be less free volume in the commercial system compared with the model system. The same phenomenon has been reported by studying glass bead-epoxy composites [22]. The linearity (Fig. 5.4) shows the activation energy is identical for each epoxy system, implying that the collective energy barrier of moisture diffusion is very close in this temperature range.

Table 5-1 Diffusion coefficient and activation energy at different temperatures.

	Diffusion Coefficients (10^{-9} cm^2/sec)				E_D
System	22°C	31°C	40°C	49°C	(kJ/mol)
Model	1.02	1.87	3.71	6.93	53
Commercial	0.99	1.39	3.24	n/a	50

Fig. 5.5 shows the change of weight gains during water immersion for both systems. After reaching the saturated moisture level, the model system samples were put into 95% R.H. condition at 22°C and 49°C, individually; the commercial system samples were put into 95% R.H. condition at 22°C and 40°C correspondingly. The drop of the moisture content after one day is negligible, since this saturated moisture absorption level is the steady state of the moisture absorption at the same level of relative humidity.

In summary, Fick's Second Law seems to fit well for the diffusion behaviors of both epoxy systems at the initial stage. The divergences in the intermediate transition

region can be explained by the previous study [14]. Most important of all, the saturated moisture level will be taken as the level of the "wet condition" to study the moisture effect on the viscoelastic performances of the epoxy adhesives. The undesired effects of water loss from epoxy adhesives during the experiments can be eliminated because of the similarity of imposed humid surroundings. Then, it can also allow us to extend the experiment time for study both systems with saturated moisture absorption.

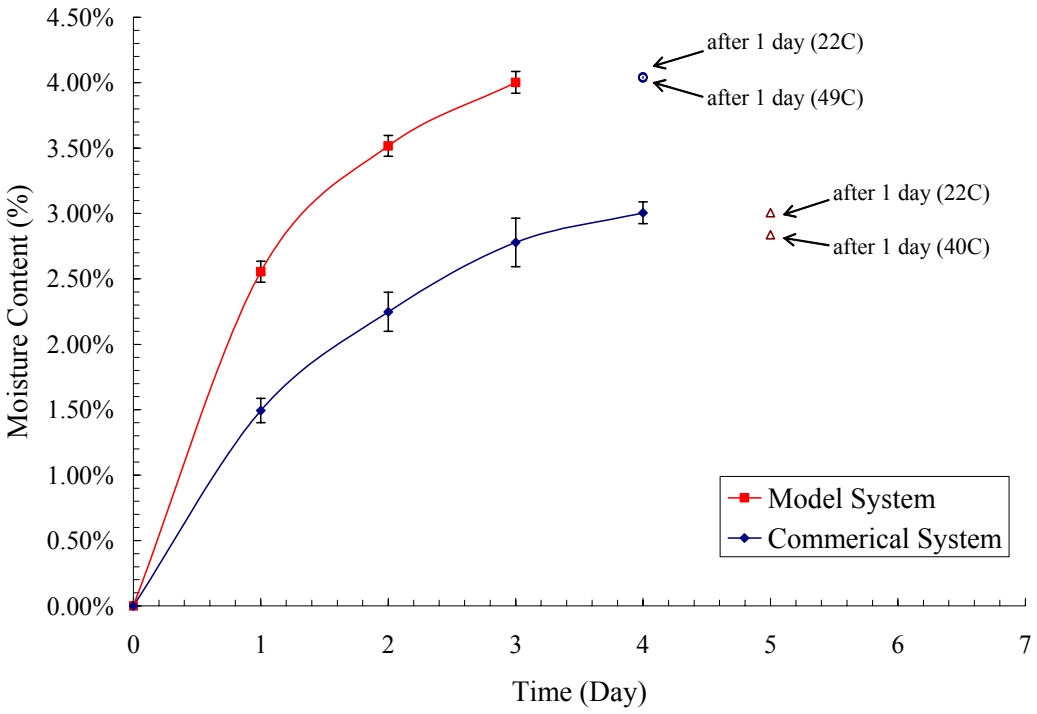

Fig. 5.5. The moisture weight gain (%) during the water immersion test; the arrows indicates weight gains in exposure to 95% R.H. environment at different temperatures.

FTIR Test Result

Fig 5.6 shows the absorbance spectra of the fully cured model and commercial epoxy system. The FTIR spectra showed that the peak at 910 cm^{-1}, which is the characteristic peak for the epoxide groups, was not observed. It confirms again that each system is in the fully cured state. Also, the relative magnitudes of the main characteristic peaks for each system are very similar, apparently indicating that the model epoxy system has a base formulation of the commercial adhesive.

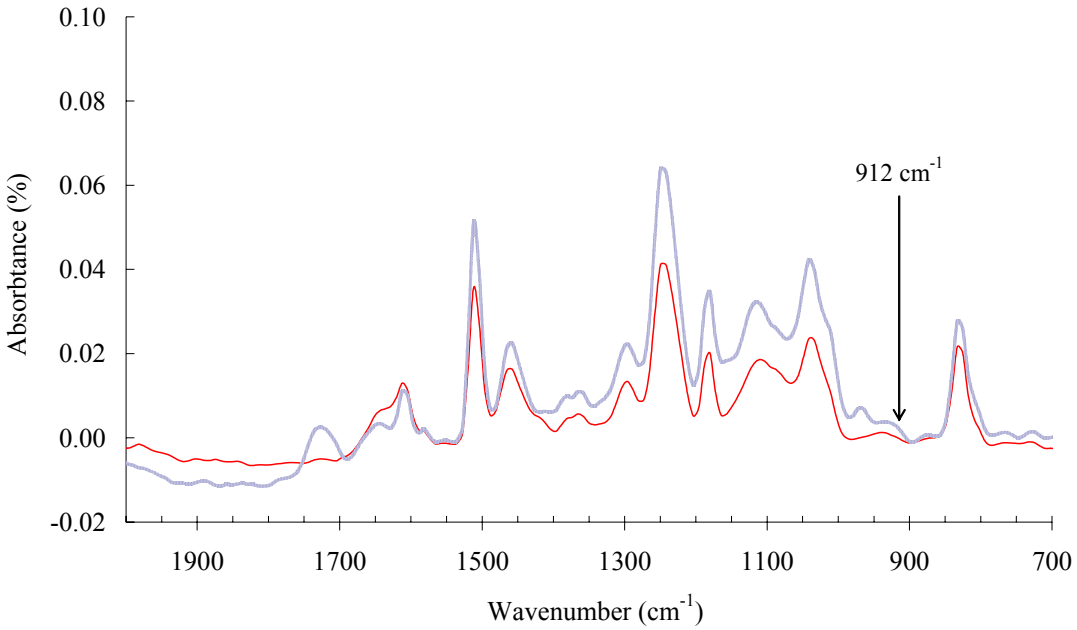

Fig. 5.6. FTIR spectra for model (solid line) and commercial (dashed line) epoxy resin systems after fully cured.

To reach the saturated moisture level, both epoxy systems were immersed into deionized water. In order to monitor any possible chemical reaction during this process, the Attenuated-total-reflectance FTIR (ATR-FTIR) spectroscopy analysis was applied during the immersion experiment on both samples (Fig. 5.7). No unexpected chemical reaction or degradation is found to take place during the water immersion tests since no change in characteristic peaks can be found. Besides, there is no obvious change of FTIR spectra between 3100 and 3700 cm^{-1} (OH-bond) after water immersion. This suggests that FTIR is not a sensitive tool to monitor the moisture weight gain in epoxy adhesives.

Incomplete curing in epoxy reins is not desirable as secondary curing reaction during hydrothermal exposure may render ambiguous experimental observation and misinterpretation of the results. The chemical degradation can also cause similar consequences. From the DSC and FTIR test results, we conclude that no chemical reaction takes place during the moisture exposure experiments.

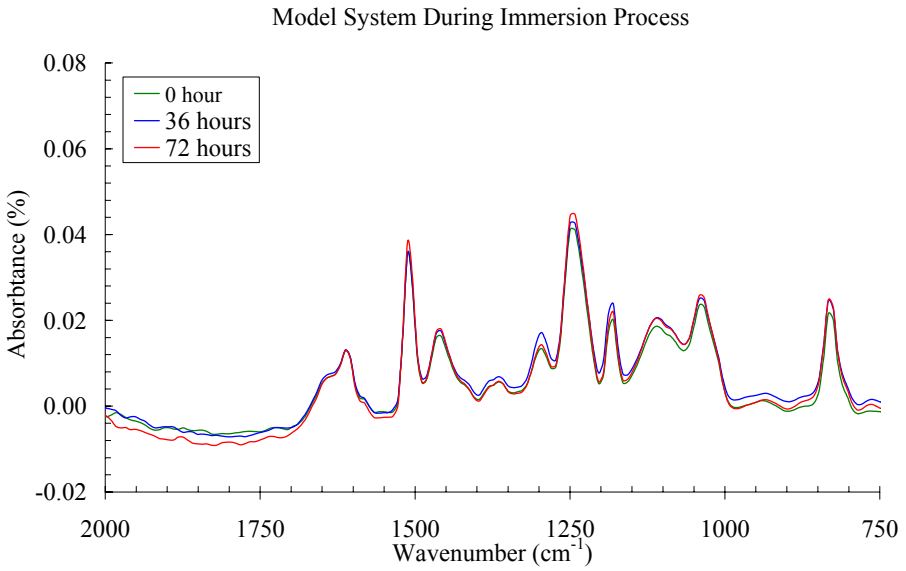

(a)

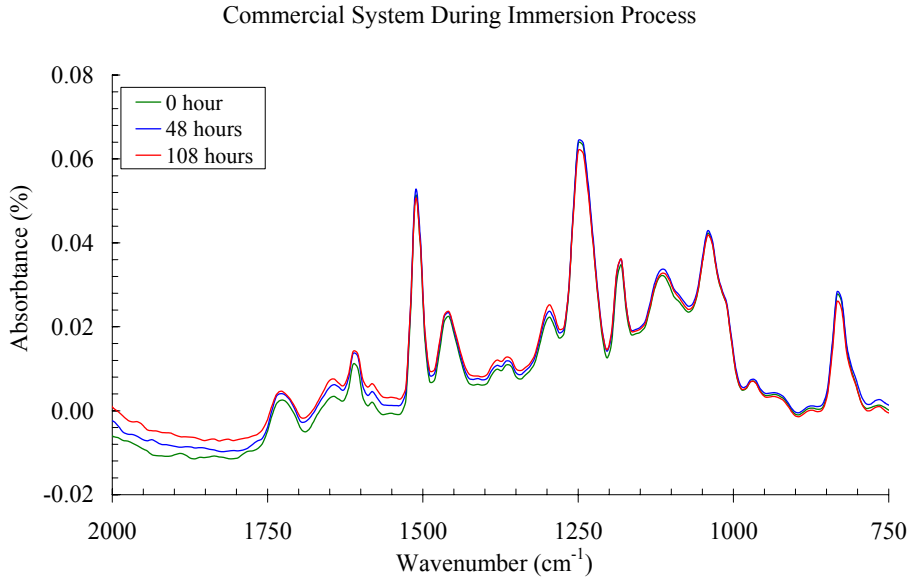

(b)

Fig. 5.7. The FTIR spectra during the moisture immersion procedures.

DMA Test Result

Dynamic Mechanical Analysis (DMA) is one of the most useful tools for investigating the viscoelastic responses of polymers. Fig. 5.8 shows the storage modulus (Pa) and the tan (δ) value under the dry and wet conditions at 1Hz in the temperature range from -90°C to 160°C. The glass and beta transition temperatures determined from the peak of the tan (δ) are listed in the Table 5-2. Also, the values of the theoretical T_g with saturated moisture level calculated from the Fox equation are also listed in Table 5-2.

$$\frac{1}{T_g^f} = \frac{W_m}{T_g^m} + \frac{W_w}{T_g^w} \tag{3.5}$$

W_w is the weight fraction of water in the matrix after water immersion test, which is 4.0% and 3.0% for model and commercial systems, respectively. This level of moisture absorption can lower the transition temperature by about 20~30°C for the epoxy systems. Besides, the broadness of the tan (δ) peak indicates the presence of small molecules (water).

The loss of absorbed water may affect the results of DMA for T_g, resulting in a misleading result compared with the theoretical T_g calculated from the Fox equation in the wet condition. A deviation of 15°C between experimental and theoretical values can be seen in the previous study [22]. One of the possible reasons is that the saturated moisture level in the previous study is the maximum absorption in the water immersions test, so that the moisture detraction may be much more aggressive with a sudden change of the surroundings, leading to a higher T_g. However, from Table 5.2,

the theoretical and experimental data show that there is a minimum water loss during the DMA experiments in our case.

The frequency sweep tests on both epoxy systems at 0.1, 1 and 10 Hz show the frequency dependence of both T_β and T_g. The activation energy value for each transition can be obtained by the Arrhenius type of relationship between frequencies, f and transition temperature, T_β, and T_g as followed:

$$f = C_\beta \exp(\frac{E_\beta}{RT_\beta}) \tag{5.2}$$

$$f = C_g \exp(\frac{E_g}{RT_g}) \tag{5.3}$$

where C_β and C_g are frequency constants; E_β and E_g is the activation energy for T_β and T_g, correspondingly, and R is the Boltzmann constant. Fig. 5.9 shows an example of the Arrhenius relationship between *log(f)* and $1/T_\beta$ in the dry condition. The linearity of each case in this plot indicates that the activation barrier corresponding to the change of frequencies is identical. In term of T_g, the derivation of the activation energy can be done in a similar way. The data are listed in the Table 5-3 based on the experimental DMA result in Fig. 5.10. The DMA has been performed on epoxy-based material (DGEBA and amines system) at 1 Hz in the previous studies. It have shown that T_β is -61°C, -57°C and the activation energy is 70, 67 kJ/mol, respectively [47, 48], which is very close to our results.

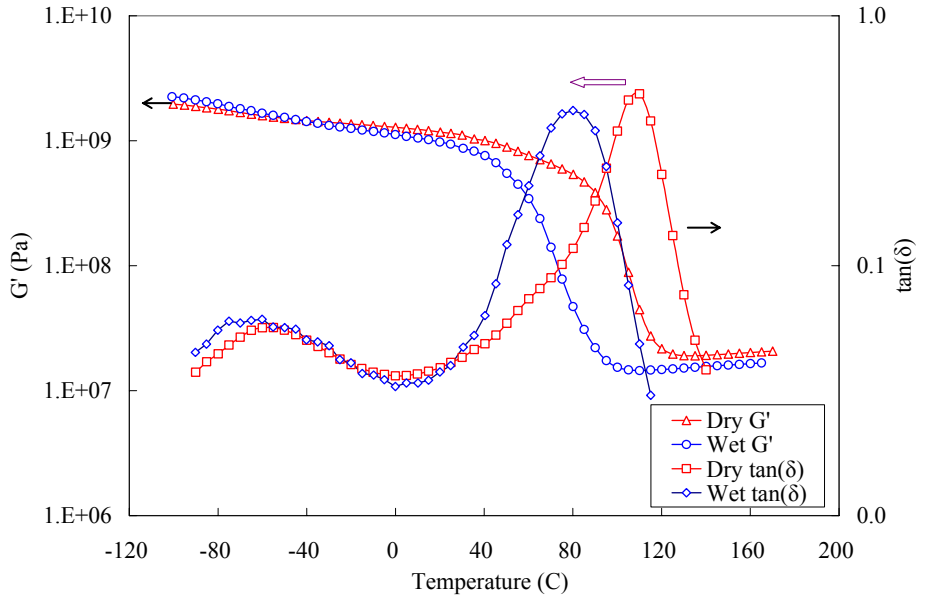

(a)

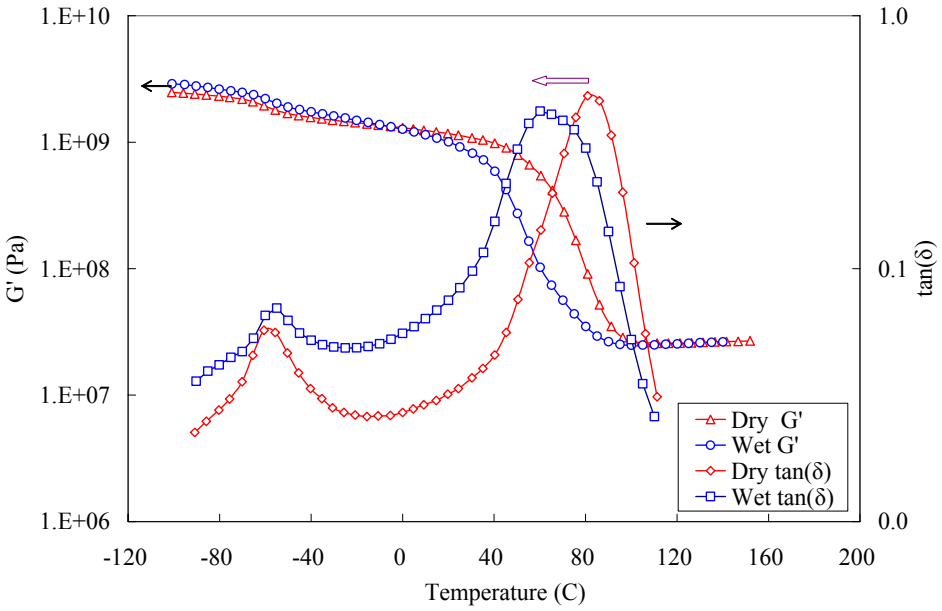

(b)

Fig. 5.8. DMA results under different conditions (a) model and (b) commercial systems.

Table 5-2 Comparison of T_g after water immersion test.

System	Glass Transition Temperature T_g (°C)		
	Dry	Wet	*Estimated by Fox Equation*
Model	110	80	*80*
Commercial	80	60	*61*

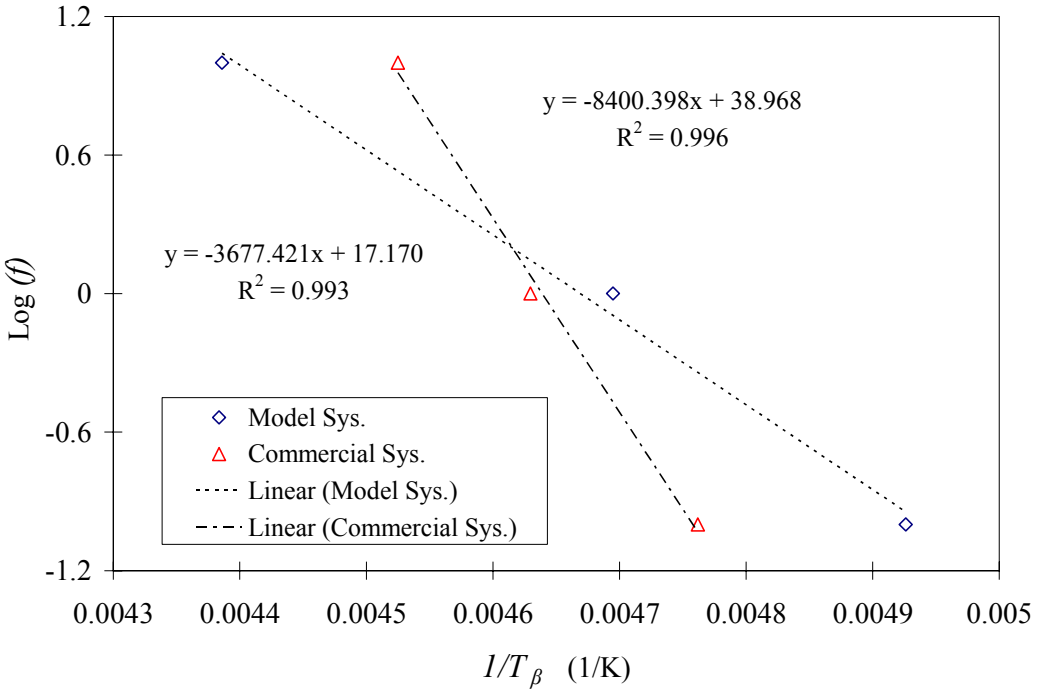

Fig. 5.9. The Arrhenius relationship between beta transition temperature and frequency in the dry condition.

Table 5-3 The transition temperature and activation energy as a function of frequency under different conditions.

(a) Beta transition temperature in the dry condition

	Beta Transition Temperature T_β (°C)			E_β
System	0.1 Hz	1 Hz	10 Hz	(kJ/mol)
Model	-70	-60	-45	70
Commercial	-63	-58	-53	180

(b) Beta transition temperature in the wet condition

	Beta Transition Temperature T_β (°C)			E_β
System	0.1 Hz	1 Hz	10 Hz	(kJ/mol)
Model	-75	-65	-50	67
Commercial	-60	-55	-50	180

(c) Glass transition temperature in the dry condition

	Glass Transition Temperature T_g (°C)			E_g
System	0.1 Hz	1 Hz	10 Hz	(kJ/mol)
Model	105	110	115	560
Commercial	75	80	90	310

(d) Glass transition temperature in the wet condition

	Glass Transition Temperature T_g (°C)			E_g
System	0.1 Hz	1 Hz	10 Hz	(kJ/mol)
Model	75	80	85	480
Commercial	50	60	65	270

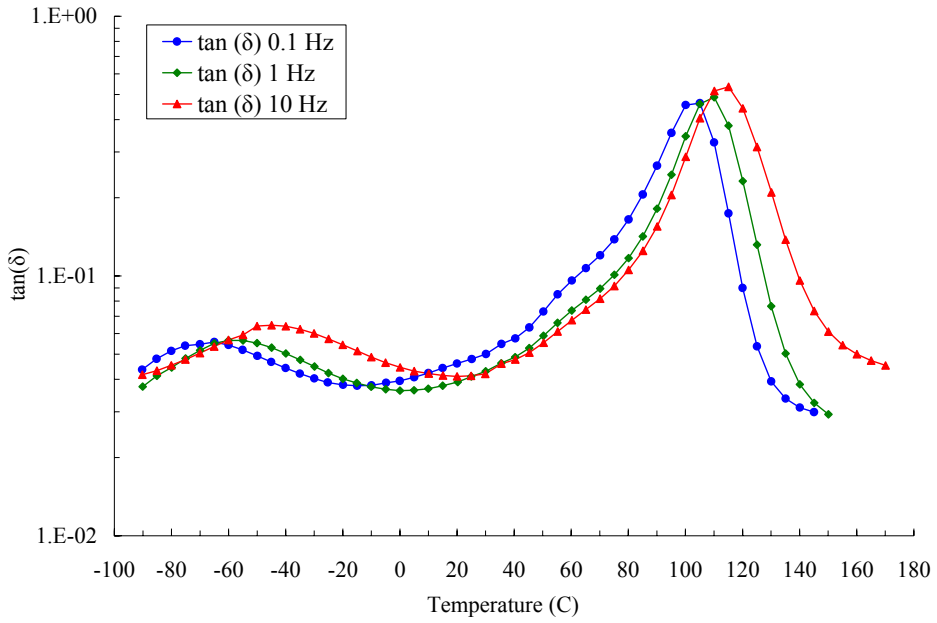

(a)

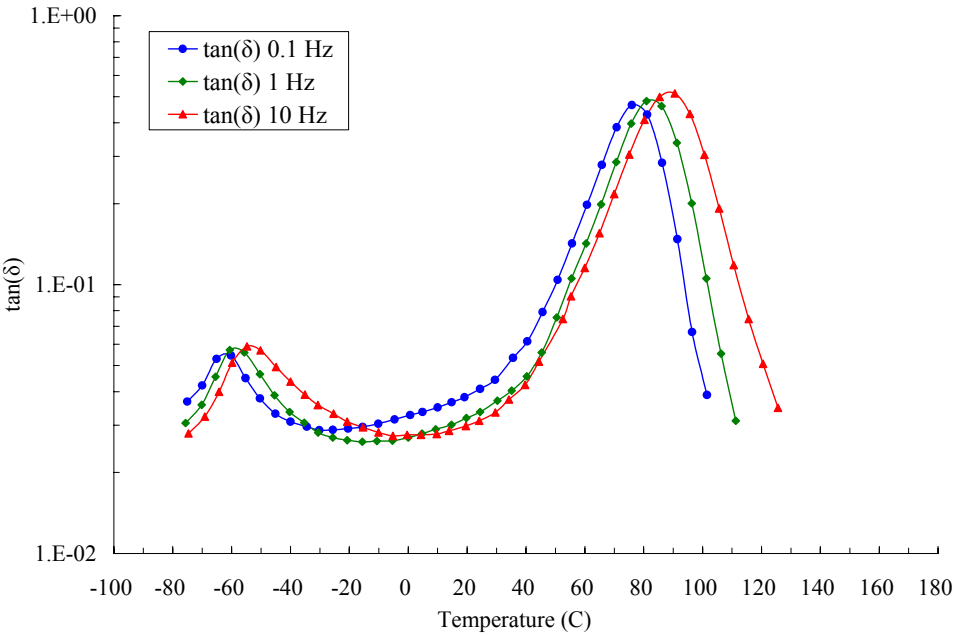

(b)

Fig. 5.10. Tan (δ) at different frequencies: (a) dry model system; (b) dry commercial system; (c) wet model system; (d) wet commercial system.

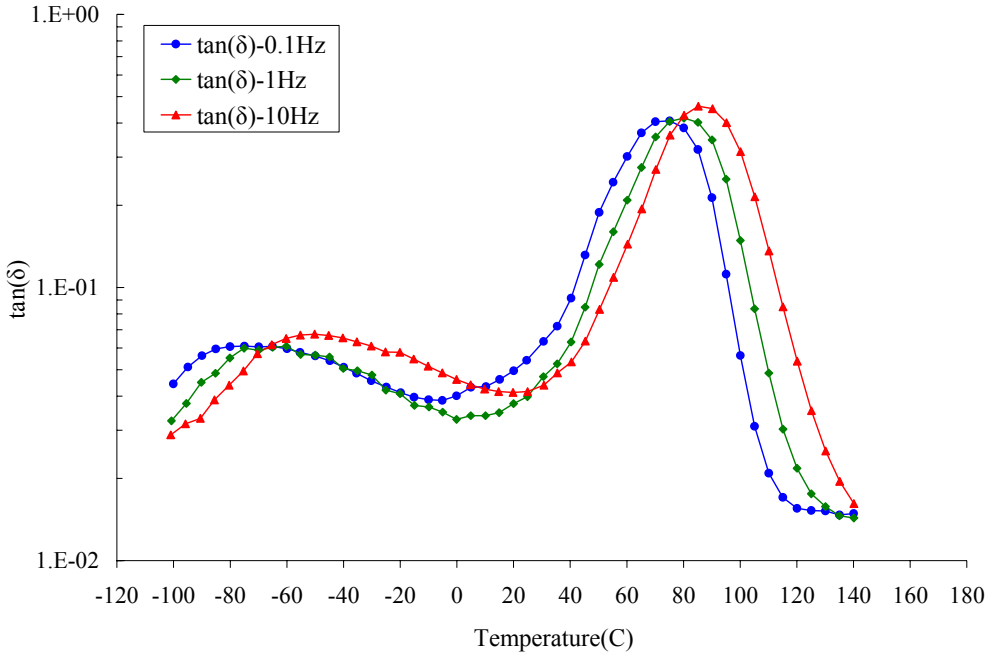

(c)

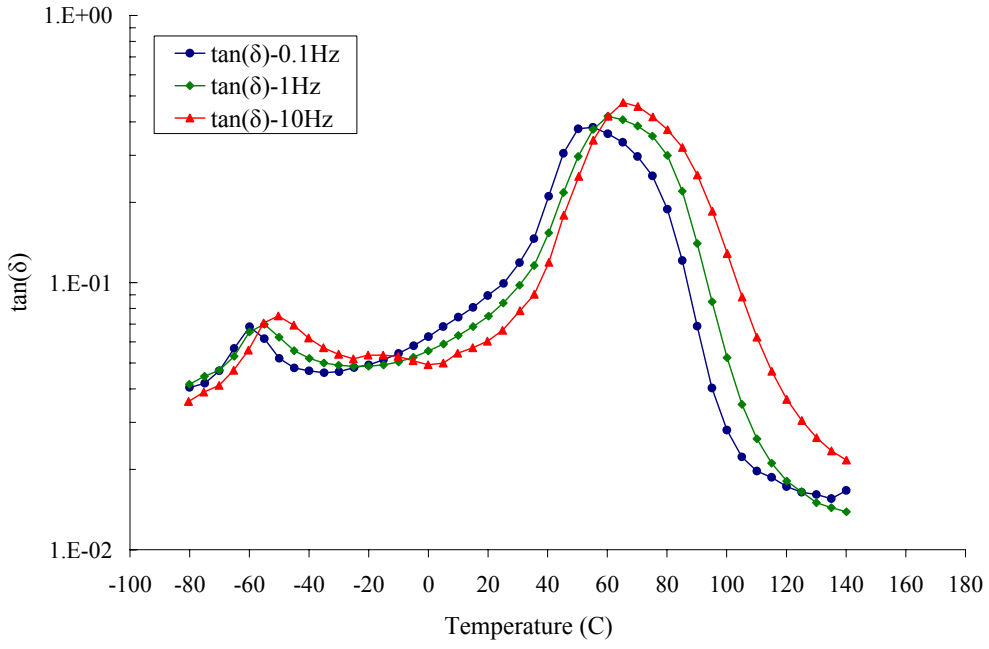

(d)

Fig. 5.10. Continued.

(1) The activation energy for the T_β is much smaller than that for the glass transition as a function of frequencies. Since the molecular behaviors in a sub-segment motion, as indicated at T_β, have a smaller energy barrier than in a cooperative long-chain segment movement, as indicated at T_g.

(2) Compared with the activation energy of T_β for both systems, a smaller sensitivity to the change of frequencies, corresponding to a larger activation energy, is found for the commercial system. One of the possibilities is the restricted molecular mobility caused by the presence of rigid fillers in the commercial epoxy system. On the contrary, the commercial system shows a smaller activation energy for T_g, which indicates that it has a higher temperature sensitivity, which may trigger a more hostile softening phenomenon at higher temperatures.

(3) Even though the presence of moisture may bring about a significant drop of T_g, the activation energy for T_β seems almost unaffected by the absorbed moisture. This may suggest that the scale of the local molecular motions may not be influenced much if it is only caused by physical interactions with water molecules. Conversely, the lower activation energy for T_g in the wet condition suggests that moisture in the matrix indeed acts as a plasticizer to cause a large scale motion or even create the micro-damages in the matrix.

Besides, the activation energy based on the frequency dependence of the T_β can be regarded as the energy barrier for sub-segmental motions of molecules, leading to the creep behavior. Normally, the polymeric chains are assumed to move in a highly localized molecular scale at temperatures below T_g. Conversely, the large scale

segmental motions are initiated above T_g. We may assume that the reflective activation energies of the collective molecular motions are similar in the temperature ranges from 22°C to 58°C for the model system and from 22°C to 36°C for the commercial system corresponding to the T_β shift in the linearly viscoelastic region. Therefore, we can apply time-temperature superposition principle in this temperature range due to the linearity in activation energy values obtained that are responsible for the corresponding molecular motions.

Creep Test Result

In Fig. 5.11 (a), the individual creep curves of the dry model system are the momentary results during the one-day isochronous experiments. Since the curves lie approximately parallel to each other in a manner, it can allow them to form a master curve. Fig. 5.11 (b) was created as a master curve by shifting each creep curve to 22°C and the solid curve represents the best fitting curve by using Coupling model (to be discussed later). The formation of the master curve indicates that an increase in temperature creates an effect that is comparable to an increase in a time scale. That is, it demonstrates that time-temperature superposition (thermo-rheological simplicity) is applicable to the creep compliance as long as deformation remains within the linearly viscoelastic range. Besides, Figs. 5.12 and 5.13 show the master curve of dry commercial system and wet model system, respectively.

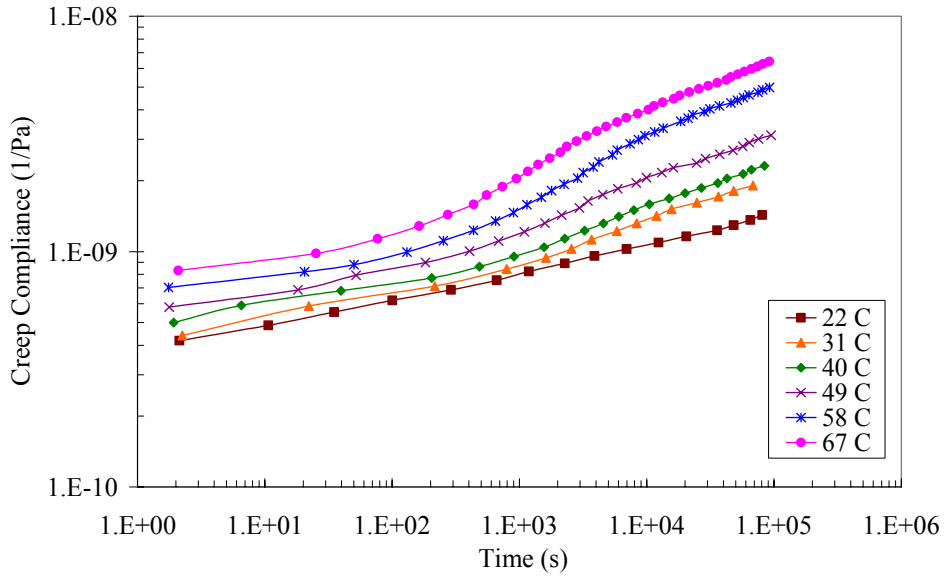

(a)

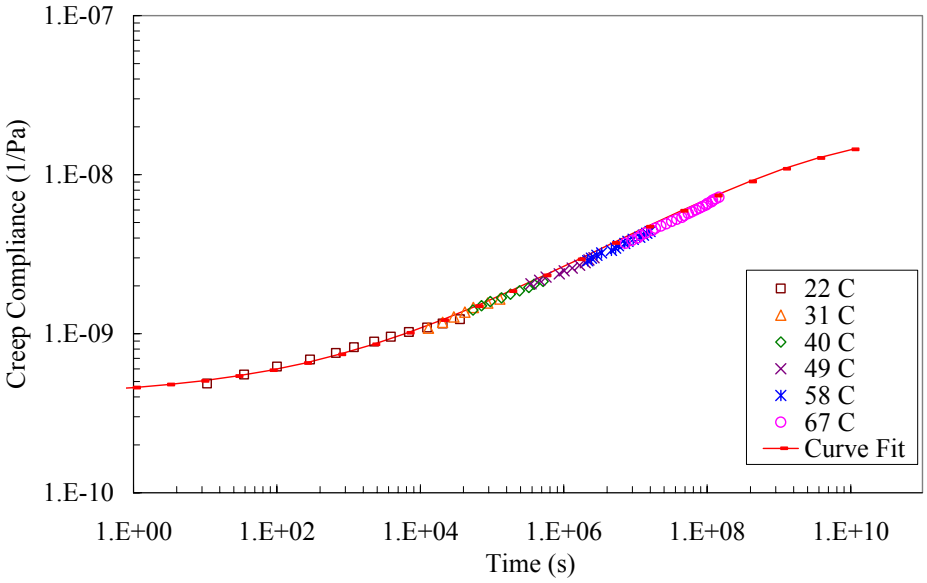

(b)

Fig. 5.11. The creep curves of model systems; (a) individual creep curves and (b) the master curve at 22°C in the dry condition.

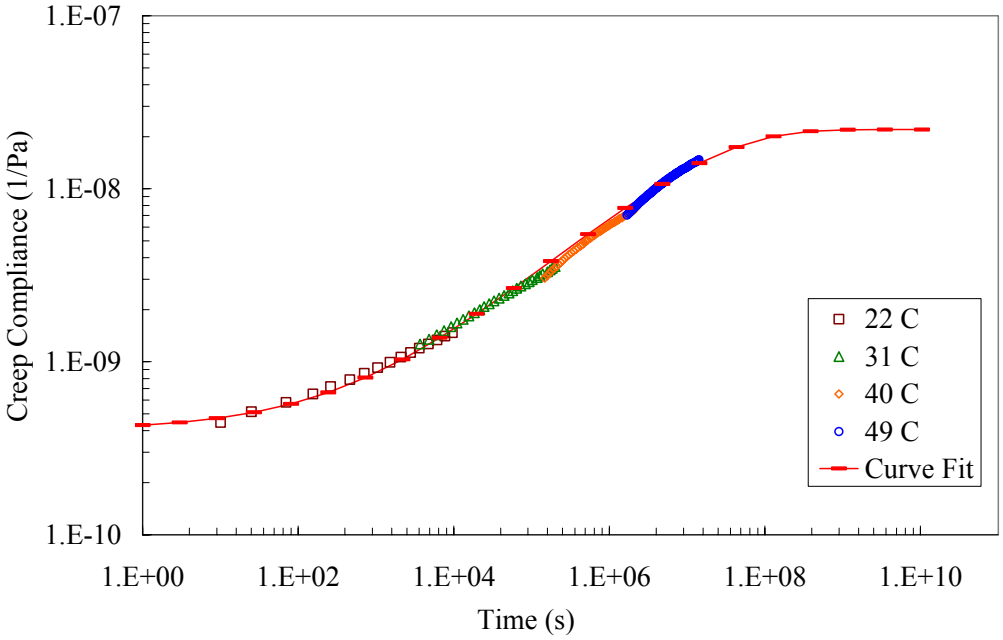

Fig. 5.12. The master curve of commercial system at 22°C in the dry condition.

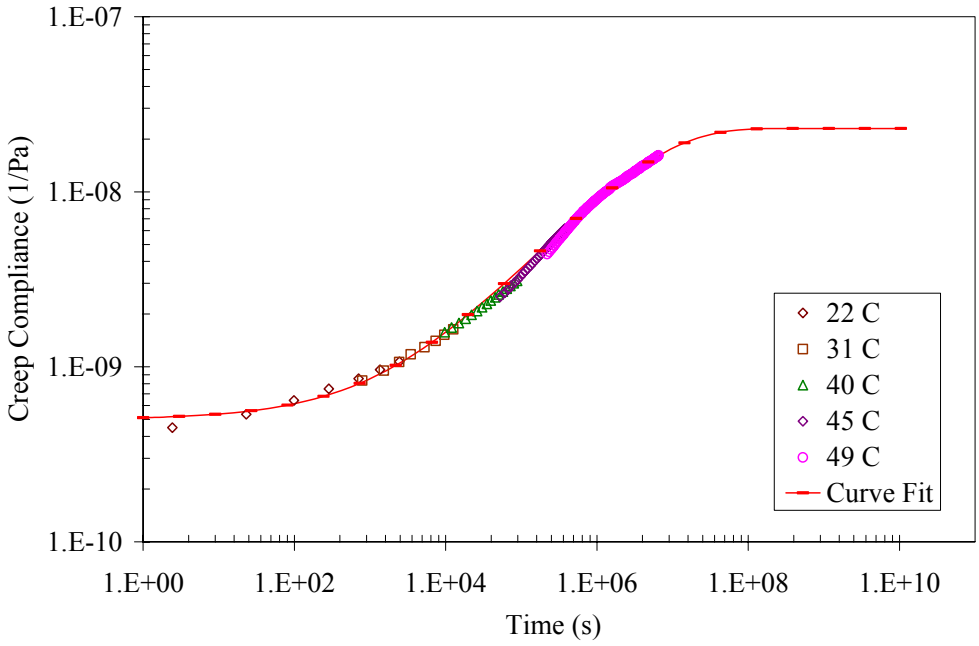

Fig. 5.13. The master curve of model system at 22°C in the wet condition.

Table 5- 4 Parameters of coupling model for master curves.

System	D_0 (10^{-8} Pa^{-1})	D_e (10^{-8} Pa^{-1})	τ^* (second)	n
Model-Dry	0.04	1.75	1.4×10^9	0.73
Model-Wet	0.05	2.30	4.7×10^6	0.51
Com.-Dry	0.04	2.20	1.4×10^7	0.60

.

Table 5-4 lists the parameters used in the Coupling model for each master curve. The initial and infinite compliances are derived from the tensile and DMA results as mentioned in previous chapter. The elastic moduli obtained from the tensile tests and the rubbery plateau moduli obtained from DMA tests are utilized for determining the compliance values of the epoxy adhesive systems when time approached to zero and infinity. The good curve-fitting results indicate that the Coupling model is capable of describing the creep behaviors of the model and commercial epoxy systems. The smaller *n* of the model system in the wet condition suggests that the water in the matrix, causing a loosening molecular constraint, which can accelerate the creep behavior. Similarly, the smaller *n* value of the dry commercial epoxy system indicates that this system has a weaker creep resistance than the model epoxy system. The presence of additives (flexibilizers and inorganic fillers) in the commercial epoxy system may contribute to this behavior.

The relationship on how the relative shift factor, A_T, change with temperature has also been shown in the Fig. 5.14. Below T_g, the value of the shift factor is often found to relate to Arrhenius type relationship based on the reference temperature, T_R:

$$\log A_T = 0.434(\frac{E_a}{R})(\frac{1}{T} - \frac{1}{T_R}) \tag{5.4}$$

where E_a is apparent activation energy (Fig. 5.14), T is testing temperature and R is the Boltzmann constant. The temperature is expressed by an absolute temperature unit in this relationship.

The linearity from the plot of the log-scale shift factors and the reciprocal of temperatures again indicates that there is a thermo-rheological simplicity based on the same apparent activation energy. Compared with the activation energy of the beta transition temperatures obtained from the DMA test, we found the same trends in the apparent activation energy here even though the values are not the same. First, the apparent activation energy of model system is found to be similar for the creep phenomena whether or not it reaches the moisture saturated level. Second, the apparent activation energy value of the commercial system is lager than that of the model system. These trends imply that there is a correlation between the activation energy of sub-segmental molecular motion (T_β) and the isochronous responses in the linearly viscoelastic region.

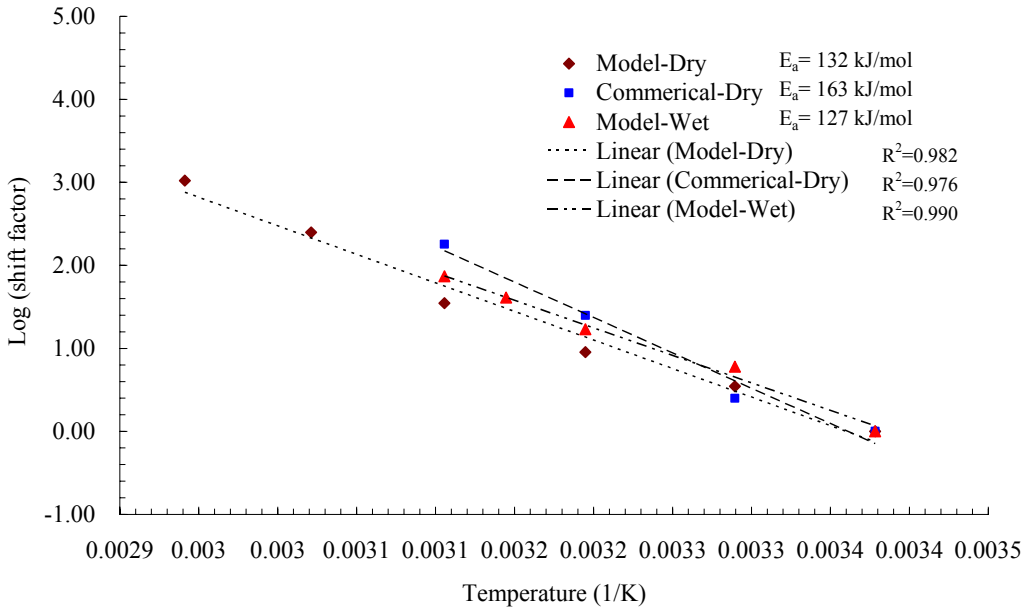

Fig. 5.14. The Arrhenius relationship between temperatures and shift factors.

The creep behavior of the commercial epoxy system in the wet condition is not reported due to its nonlinearly viscoelastic response even at low temperatures, e.g., 30°C. As a result, the creep compliance curve of the commercial epoxy system under the wet condition could not be shifted to form a smooth master curve. Furthermore, the deviation of the creep behavior in the wet condition from the Coupling model of the commercial system may be due to the non-uniform distribution of the absorbed moisture in epoxy caused by the complex formulation introduced in the commercial system.

The creep compliance of the commercial epoxy system by curve fitting obtained from the Coupling model deviates from the value calculated by the rubbery plateau modulus from the DMA result. This discrepancy may be attributed by the presence of the filler effects. The fillers can increase the matrix rigidity leading to a higher rubber plateau modulus of the commercial epoxy system. However, the viscoelastic behavior is mainly caused by the epoxy resin matrix during the creep tests. This phenomenon may explain why it is not effective to estimate the equilibrium creep compliance by using the rubbery plateau modulus for the commercial epoxy system.

Equivalence between Effect of Temperature and Moisture

Epoxy adhesives exhibit a more pronounced creep behavior at elevated temperatures due to a higher molecular mobility. Similarly, the presence of moisture in the epoxy systems also accelerates the creep process as shown in the previous section. When we compare individual isochronous curves under different conditions, it has been found that the model epoxy system has a similar viscoelastic response between the condition at a higher temperature in the dry condition and the condition at a lower temperature but with saturated moisture content (Fig 5.15). Fig. 5.15(a) shows the equivalence between the dry creep compliance at 62°C and the wet creep compliance at 40°C (Case I). Similarly, Figure 5.15(b) shows the equivalence between the dry compliance at 51°C and the wet compliance at 31°C (Case II). The dry creep curve at 62°C and 51°C has been shifted 1.5 and 2.0 from that at 58°C and 49°C, respectively, by following the Arrhenius' relationship (equation 5.4). Both cases show that each

group of creep curves has a perfect match, proving that the presence of absorbed moisture can bring about the same creep response in the dry condition but at a higher temperature. In Table 5-5, it shows the ratios of the testing temperature and its T_g in Kelvin scale and indicates that the model epoxy system responses at the same temperature scale based on the different T_g (dry: 110°C; wet: 80°C). This observation rationalizes the equivalence between the effect of temperature and moisture.

Table 5-5 The equivalence of temperature and moisture effect on creep behaviors and the moisture effect on T_g.

	Temperature (dry vs. wet)		$T(K)/T_g(K)$	
	Case I	Case II	Case I	Case II
Dry	62°C	51°C	0.88	0.85
Wet	40°C	31°C	0.89	0.86

As for the effect of absorbed moisture on the creep behavior, a ratio of the testing temperature (T_{wet}/T_{dry}) for wet conditions is found to be 0.93 (Case I) and 0.94 (Case II), respectively. The 4% of absorbed moisture leads to a ratio of the T_g drop, 0.92 (T_{wet}/T_{dry}). Interestingly, the ratios of the magnitudes in temperature differences for the viscoelastic creep behavior are equal to that of the T_g depression due to the absorbed water in the wet condition. That is, both thermal property (T_g) and mechanical property (creep compliance) can reveal the temperature-moisture equivalence between dry and wet condition by this quantitative analysis.

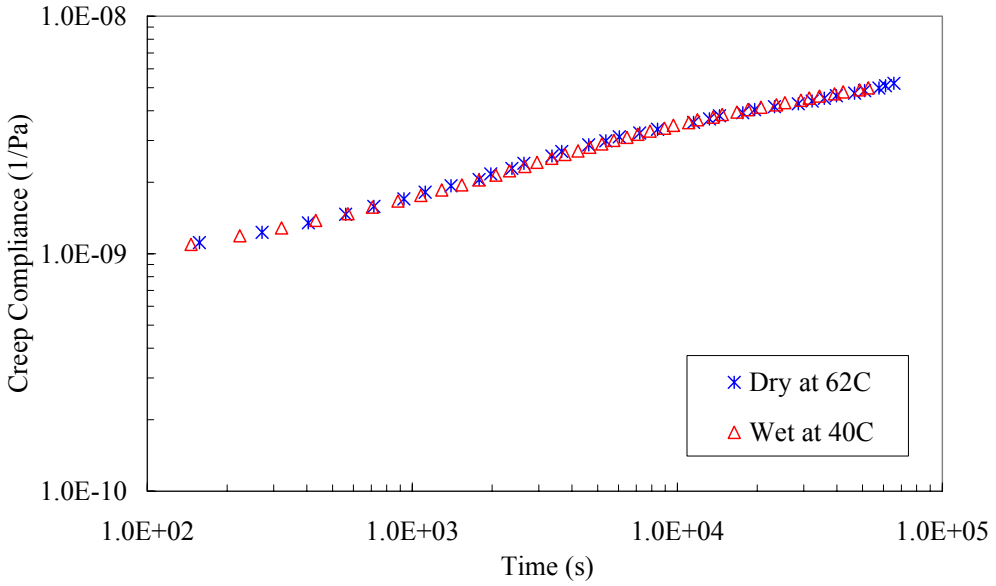

(a)

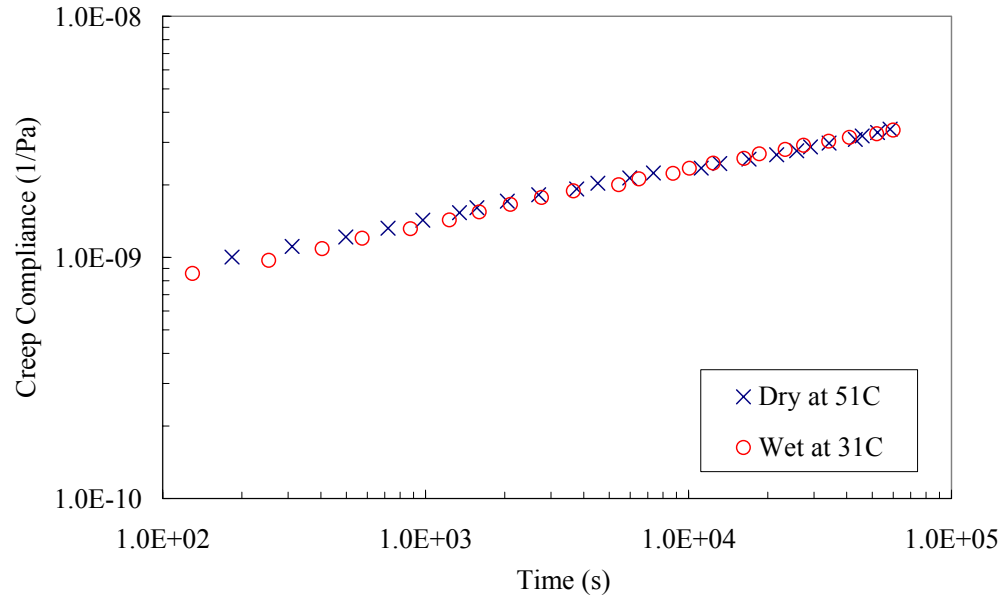

(b)

Fig. 5.15. The equivalence of temperature and moisture effect on creep curves.

In summary, the creep behaviors of a model epoxy adhesive and a commercial epoxy adhesive have been investigated in the linearly viscoelastic region in this study. The temperature and moisture effects were also emphasized to correlate with the mechanical responses. Water immersion experiments are found to be a viable method to accelerate the moisture uptake to reach saturated moisture levels. Based on the previous moisture diffusion experiments, the saturated moisture absorption level in the humid environments, reached by the accelerated immersion tests, can avoid the loss of water content during testing. This method can allow us to extend the time period of creep tests in the wet condition.

DSC and FTIR techniques were utilized to monitor the possible occurrence of chemical reaction or degradation for the fully-cured epoxy adhesives during testing. The results of tensile and DMA tests indicate that a small amount of the absorbed moisture could greatly reduce the mechanical properties. The time-temperature superposition principle is found to be applicable for both epoxy systems in the linearly viscoelastic region and the shift factors as a function of temperature obey the Arrhenius relationship, which allows us to construct a creep compliance master curve in the regions below T_g. The Coupling model can successfully fit the creep master curves in both dry and wet conditions. Also, the other parameters in the model can be reasonably derived from the elastic moduli and rubbery plateau moduli. The physics-based Coupling parameter, n, which corresponds to the constraint of molecular mobility, is useful for describing the state of molecular mobility of epoxy adhesives. Furthermore, the equivalence of the temperature and moisture on their influence of creep behavior is

found to correlate quantitatively in the model epoxy adhesive system. This allows us to predict the creep behavior under the effect of moisture by applying dry creep curves at a higher temperature based on the equivalent effect of temperature and moisture.

CHAPTER VI

CONCLUSION

A methodology has been established to study the long-term creep phenomena of epoxy adhesives under different environmental conditions. Because of the complex composition of the commercial adhesives, a model epoxy system has been studied simultaneously as a reference material system. The moisture diffusion behavior has been investigated by a series of long-term moisture diffusion tests. Then, accelerated moisture absorption has been performed via water immersion to reach the saturated moisture absorption. Only physical interactions between moisture and epoxy were found during the immersion process. The tensile and DMA tests were performed at different temperature and moisture levels. The results suggest that moisture absorption exhibits a more noticeable effect at high temperatures near the glass transition regime. Compared with the model epoxy system, the commercial epoxy system shows a weaker creep resistance at elevated temperatures or under moisturized environment.

The time-temperature superposition principle is found to be applicable for both epoxy systems in the linearly viscoelastic region. The Coupling model can successfully fit the creep master curves in both dry and wet conditions. The physics-based Coupling parameter, n, which corresponds to the constraint of molecular mobility, can describe well the state of molecular mobility of epoxy adhesives. The same trend is found for the activation energy for the beta transition temperatures (DMA) and the creep shift factors whether or not it has moisture present, indicating that water molecules may have a minor influence on local molecular motions. However, the

presence of water molecules inside the adhesive systems can indeed lower T_g, constricting the temperature range for applications. The equivalence between the effect of temperature and moisture on the creep behavior is quantitatively established. Also, a correlation of the drop of T_g and creep responses is addressed accordingly.

The significance of this research is therefore seen as providing a methodology to study the creep behavior of epoxy adhesives under different environmental effects, even though the analysis complexity may increase with the presence of different additives or fillers in the matrix. Besides, the quantitative correlation of moisture and temperature effect may allow us to predict the creep behavior under the effect of moisture by only studying the dry creep behavior at a higher temperature if the T_g depression of the epoxy adhesives due to moisture uptake can be determined.

REFERENCES

[1] A. J. Kinloch, Adhesion and Adhesives, Chapman and Hall, New York, 1987.

[2] J. D. Ferry, Viscoelastic Properties of Polymers, 3rd ed., Wiley, New York, 1980.

[3] O. Olabisi, L. M. Roberson and M. T. Shaw, Polymer-Polymer Miscibility, Academic Press, New York, 1979.

[4] P. C. Powell, Engineering with Polymers, Chapman and Hall Academic, New York, 1983.

[5] J. Raghavan and M. Meshii, Composites Sci. and Tech., 57 (1997) 1673

[6] E. M. Woo, Composites, 25 (1993) 425.

[7] A. Sen, M. Bhattacharya, K. A. Stelson and V.R, Mater. Sci. and Eng. A, 338 (2002) 60.

[8] D. J. O'Brien, P. T. Mather and S. R. White, J. Composite Materials, 35 (2001) 883.

[9] P. A. O'Connell and G. B. McKenna, J. of Chemical Physics, 110 (1999) 11054.

[10] A. Apicella, R. Tessieri and C. D. Cataldis, J. Membr. Sci. 18 (1984) 211.

[11] J. Crank and G. S. Park, Diffusion in Polymers, Academic Press, New York, 1968.

[12] J. Zhou and J. P. Lucas, Polymer, 40 (1999) 5505.

[13] Y. Diamant, G. Marom, and L. J. Broutman, J. Appl. Polymer Sci., 26 (1981) 3015.

[14] C. L. Soles, F. T. Chang, D W. Gidley and A. F. Yee, J. Polymer Science: Part B, 38 (2000) 776.

[15] J. Zhou and J. P. Lucas, Composites Science and Technology, 53 (1995) 57.

[16] Y. Li, J. Miranda and H.-J. Sue, Polymer, 42 (2001) 7791.

[17] M. Fernandez-Garcia and M. Y. M. Chiang, J. Applied Polymer Science, 84 (2002) 1581.

[18] C. H. Shen and G. S. Springer, Composite Mater., 11 (1977) 2.

[19] C. H. Shen and G. S. Springer, Composite Mater., 11 (1977) 250.

[20] D. M. Brewis, J. Comyn, A. K. Raval and A. J. Kinloch, Int. J. Adhesion and Adhesives, 10 (1990) 247.

[21] F. U. Buehler and J. C. Seferis, Composites: Part A, 31 (2000) 741.

[22] J. Y. Wang and H. J. Ploehn, J. Applied Polymer Science, 59 (1996) 245.

[23] M. Woo and J. Piggot, J. Composites Technology & Research, 9 (1987) 101.

[24] R. J. Crowson and R. G. C. Arridge, Polymer, 20 (1979) 737.

[25] T. S. Chow, Polymer, 29 (1988) 1447.

[26] G. B. Mckenna and R. J. Haylord, Polymer, 29 (1988) 2027.

[27] M. Al-Haik, M. Vaghar, H. Garmestani and M. Shahaway, Composites: Part B, 32 (2001) 165.

[28] J. M. Augl, J. Rheology, 31 (1987) 1.

[29] I. M. Ward and D. W. Hadley, An Introduction to the Mechanical Properties of Solid Polymers, Wiley, New York, 1993.

[30] L. E. Nielsen and R. F. Landel, Mechanical properties of polymers and composites, Marcel Dekker, New York, 1994.

[31] F. Pang and C. H. Wang, Composites: Part B, 30 (1999) 613.

[32] F. Li, R. C. Larock and J. U. Otaigbe, Polymer, 41 (2000) 4849.

[33] R. Kohlrausch, Ann. Phys. Chem. J. C. Poggendorff, 191 (1854) 179.

[34] G. Williams and D. C. Watts, Trans. Faraday Soc., 66 (1970) 80.

[35] K. L. Ngai and C. T. White, Physical Review B, 20 (1979) 2475.

[36] K. L. Ngai, A. K. Johscher and C. T. White, Nature, 277 (1979) 185.

[37] K. L. Ngai, D. J. Plazek and R. W. Rendell, Rheol Acta, 36 (1997) 307.

[38] K. L. Ngai, Y.-N. Wang and L. B. Magalas, J. Alloys and Compounds 211/212 (1994) 327.

[39] R. W. Rendell, K. L. Ngai, G. R. Fong, A. F. Yee and R. J. Bankert, Polymer Engineering and Science 27 (1987) 1.

[40] D. J. Plazek and K. L. Ngai, Macromolecules, 24 (1991) 1222.

[41] C. M. Roland, K. L. Ngai and D. J. Plazek, Comp. and Theor. Polym. Sci., 7 (1997) 133.

[42] D. G. Hunt, Polymer, 20 (1979) 241.

[43] R. M. Guedes, J. J. L. Morais, A. T. Marques and A. H. Cardon, Computers & Structures, 76 (2000) 183.

[44] L. H. Sperling, Introduction to Physical Polymer Science, 3rd ed., John Wiley & Sons, New York, 2001.

[45] V. F. Janas and R. L .McCullough, Composites Science and Technology, 30 (1987) 99.

[46] K. Nakamura K, T. Maruno and S. Sasaki, Int. J. Adhesion and Adhesives, 7 (1987) 97.

[47] L. Heux, J. L. Halary, F. Laupretre and L. Monnerie, Polymer, 38 (1997) 1767

[48] S. Cukierman, J.-L Halary and L. Monnerie, J. non-crystalline Solids, 131-133 (1991) 898.

VITA

Chih-Wei, Feng was born in Chunghua, Taiwan on January 15, 1977. In June of 1995, Chih-Wei graduated from MingDao High School, Taiwan. He continued his education at National Taiwan University in the Department of Mechanical Engineering. In June of 1999, he graduated with a Bachelor of Science degree in mechanical engineering and a minor in economics.

After school, Chih-Wei went to serve as a Second Lieutenant of Artillery in the Army for two years. Then, he worked in the semiconductor packaging industry for one year before came to Texas A&M University for further study. At A&M, he works as a research assistant in the Polymer Technology Center.

Chih-Wei's permanent address follows:

25 Lane16 Huayang St.

Chunghua City, 500

Taiwan, R.O.C.